Physics Reports 510 (2012) 87–118

Contents lists available at SciVerse ScienceDirect

Physics Reports

journal homepage: www.elsevier.com/locate/physrep

Stochastic theory of nonequilibrium steady states. Part II: Applications in chemical biophysics

Hao Ge [a], Min Qian [b], Hong Qian [c,*]

[a] School of Mathematical Sciences and Centre for Computational Systems Biology, Fudan University, Shanghai, 200433, PR China

[b] School of Mathematical Sciences, Peking University, Beijing, 100871, PR China

[c] Department of Applied Mathematics, University of Washington, Seattle, WA 98195, USA

ARTICLE INFO

Article history:
Accepted 21 August 2011
Available online 17 September 2011
editor: H. Orland

Keywords:
Enzyme kinetics
Fluctuating enzyme
Gene regulatory network
Kinetic proofreading
Signaling network
Zeroth-order ultrasensitivity
Bistability

ABSTRACT

The mathematical theory of nonequilibrium steady state (NESS) has a natural application in open biochemical systems which have sustained source(s) and sink(s) in terms of a difference in their chemical potentials. After a brief introduction in Section 1, in Part II of this review, we present the widely studied biochemical enzyme kinetics, the workhorse of biochemical dynamic modeling, in terms of the theory of NESS (Section 2.1). We then show that several phenomena in enzyme kinetics, including a newly discovered activation–inhibition switching (Section 2.2) and the well-known non-Michaelis–Menten-cooperativity (Section 2.3) and kinetic proofreading (Section 2.4), are all consequences of the NESS of driven biochemical systems with associated cycle fluxes. Section 3 is focused on nonlinear and nonequilibrium systems of biochemical reactions. We use the phosphorylation–dephosphorylation cycle (PdPC), one of the most important biochemical signaling networks, as an example (Section 3.1). It starts with a brief introduction of the Delbrück–Gillespie process approach to mesoscopic biochemical kinetics (Sections 3.2 and 3.3). We shall discuss the zeroth-order ultrasensitivity of PdPC in terms of a new concept — the temporal cooperativity (Sections 3.4 and 3.5), as well as PdPC with feedback which leads to biochemical nonlinear bistability (Section 3.6). Also, both are nonequilibrium phenomena. PdPC with a nonlinear feedback is kinetically isomorphic to a self-regulating gene expression network, hence the theory of NESS discussed here could have wide applications to many other biochemical systems.

Contents

* Corresponding author.
E-mail addresses: edmundge@gmail.com (H. Ge), qianpku@gmail.com (M. Qian), hqian@u.washington.edu (H. Qian).

0370-1573/$ – see front matter © 2011 Elsevier B.V. All rights reserved.
doi:10.1016/j.physrep.2011.09.001

1. Introduction to Part II

In Part I, we have presented a general theory for the nonequilibrium steady state (NESS) of stochastic, Markovian dynamics. Two applications of this general theory were discussed: the coherence resonance in stochastic nonlinear systems (Section 3 of Part I) and the unidirectional motion and efficiency of molecular motors (Section 4 of Part I). In this Part II, we shall discuss two more applications, in molecular biophysics and chemical biophysics: the single-molecular enzymology with linear kinetics (Section 2) and the nonlinear phosphorylation–dephosphorylation cycle kinetics for cellular signaling (Section 3). We shall start Part II with an introduction of its own with a brief recap of the essentials from Part I and some introductory remarks on biochemical applications. Part II ends with some additional remarks on the development of the theory of NESS from the authors' perspective.

1.1. The theory of nonequilibrium steady states

The NESS theory is a theory about any stochastic systems that endowed with a Markovian dynamics. Just as attractors are fundamental to the understanding of any deterministic dynamics, the NESS is the long-time, stationary behavior of a wide class of stochastic systems with recurrence and irreducible. In the classical deterministic dynamics, a distinction between equilibrium steady states and nonequilibrium steady states was never formally made. They are all called fixed points (or attractors in a broader sense). After all, the concept of equilibrium only rises in statistical physics. Exactly being inspired by the physics, the NESS theory makes a fundamental distinction between the two types of stationary states, or more precisely stationary processes, in stochastic dynamical systems.

It turns out, there are great manifestations from making this distinction, with deeper understandings and new insights emerging naturally.

First, one can clearly associate an equilibrium with *time reversibility*, in a statistical sense, in the forward stationary dynamics and its time reversal, i.e., a recording played backward. Furthermore, to quantify the time irreversibility associated with a NESS, a concept of *entropy production rate* is introduced based on the measure-theoretical distance between the forward and reversed processes. In applications to molecular physics, this mathematically defined entropy production rate matches precisely what physicists and chemists have conceived, off by a unit of k_BT. Note that the concept of entropy production rate does not exist in the standard theory of equilibrium physics; It only exists in the various forms of nonequilibrium, irreversible thermodynamics that still lack a unified narrative.

Second, the time-reversal symmetry implies certain self-adjoint property in the time-evolution operator of a Markov process. In the case of discrete state Markov chain, this turns out to be the celebrated *detailed balance condition*. Furthermore, the detailed balance condition implies a "gradient-like" potential function in the underlying dynamics. Therefore, stochastic dynamical systems that approach to equilibrium steady states have to satisfy certain conditions: This had been realized for a long time in physics [1,2] and chemistry [3,4], but was first firmly established mathematically by Kolmogorov [5].

Third, for a system that approaches to a NESS, because of the lack of detailed balance and potential condition, it naturally exhibits circular motion. The stationarity, in this case, is maintained not by detailed balance, but circular balance. From a physics and chemistry standpoint, such a system requires a sustained *external driving force*; it has to be open to its environment in a significant way. When the driving force is sufficiently large, the stochastic circular motion emerges as macroscopic oscillations. Here we see why coherence resonance is intimately related to a NESS.

Finally, because of the dynamics of a system that approaches to a NESS is non-gradient-like, it dissipates energy with every cyclic motion. It turns out, this dissipation is exactly the origin of positive entropy production rate in a NESS. The efficiency of a molecular motor, thus, can be rigorously studied in terms of the theory of NESS.

1.2. Nonequilibrium steady states in chemical biophysics

Biophysics and biophysical chemistry textbooks usually start either with biological macromolecules, such as proteins and DNA, or with enzymatic reaction kinetics which is the fundamental unit of biochemical reactions in living organisms. In both cases, however, the concept of discrete conformational states of a protein or enzyme is essential. Even though the conformational states of a biological macromolecule are themselves emergent properties of a *many-body* polymer system in the classical statistical mechanics, and they are the focuses of molecular biophysics based on Kramers' 1940 diffusion approach to chemical reactions [6,7], many functional aspects of biochemistry can be understood based on the empirically established concepts of *conformational states* and *allosterism* of a protein.

The above premise grants the use of discrete-state, continuous-time Markov chain, also known as master equation approach, as a meaningful mathematical representation of the state of a biomolecular system. The corresponding theory of NESS then applies. It turns out, this is the most natural way of looking at enzymatic reactions of single enzyme molecules, either in isolation as in the recently developed *single-molecule enzymology*, or in a biochemical reaction network. We shall discuss both cases, with one of the examples for the latter being the enzyme regulation by phosphorylation–dephosphorylation cycle (PdPC), catalyzed by respective kinase and phosphatase.

One of the significant insights derived from the stochastic theory of NESS is that an enzyme molecule that catalyzes a biochemical reaction in a living cell is in a NESS most of the time: Usually the concentrations of the substrate and product of an enzymatic reaction is approximately constant in a homeostatic cell. This new insight immediately eliminates the usual, painful need for establishing a "quasi-steady state" of an enzyme in the traditional theory for relaxation kinetics in test tubes. In fact, a new, stochastic derivation of the celebrated Michaelis–Menten equation becomes obvious. Furthermore, the somewhat "mysterious" Haldane's relation is nothing but a consequence of an isolated reversible enzyme reaction necessarily approaching to an equilibrium steady state.

At the meantime, in an almost effortless manner, one is able to show that why any complex enzyme kinetics, as long as there is only a single unbound enzyme species, will exhibit the Michaelis–Menten kinetics. This is a result not widely appreciated enough; even though it has been repeated discovered in the enzyme kinetic studies [8–11].

Section 2 will present the stochastic NESS theory for single-molecule enzyme kinetics. In Section 3 we study the important question of how open, driven biochemical reaction systems give rise to biochemical functions. In particle, the theory of NESS provides the recipe for quantifying the energy dissipation, which can and should be correlated with the biochemical function.

The "function" we focus on is the so-called *switching behavior*. It turns out, the amplitude of such a switch is dictated by the amount of energy drive, usually in the form of ATP hydrolysis in a cell. We also discover that the sharpness of the switching transition, which reflects a novel form of cooperativity, is also a consequence of the open-system nature of PdPC.

The in-depth study of PdPC is made more significant due to the realization that it is kinetically isomorphic to another widely used biochemical signaling system called GTPase. Furthermore, positive feedback regulations have been widely observed in cell biology. By augmenting the simple PdPC (or GTPase) that consists only two biochemical reactions with an extra step of binding, the switch becomes bistable. We then show that this PdPC with feedback is kinetically identical to the genetic networks with self-regulating genes. One can find a series of studies of this subject in [12–15]. Therefore, the stochastic NESS study of PdPC provides a prototype for modeling many complex biochemical reaction networks in cellular biology.

2. Applications to single-molecule enzyme kinetics

There is a resurgence of interests in the theory of enzyme kinetics due to several recent developments in biochemical research: The foremost is the systems approach to cell biology which demands quantitative characterizations of cellular enzymatic reactions in terms of Michaelis–Menten (MM) like kinetics. Second, recent advances in single-molecule enzymology have generated exquisite information on protein dynamics in connection to enzyme catalysis [16–19]. And third, the most relevant one to the present review, is the theoretical advance in our understanding of open, driven biochemical reaction systems in terms of the theory of nonequilibrium steady state.

Single-molecule enzymology and enzymatic reactions inside cells have shown the necessity of modeling enzyme reactions in terms of stochastic mathematics. On the theory side, an alternative to the MM approach that is particularly applicable to stochastic single-molecule enzyme kinetics has emerged. Motivated by single-molecule experiments, we shall introduce the concepts, and derive mathematical expressions, for the *cycle fluxes*, *waiting cycle times*, and *stepping*

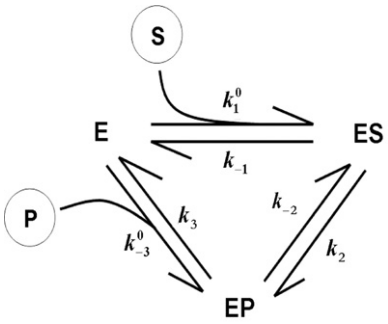

Fig. 1. Kinetic scheme of a simple reversible enzyme reaction in which k_1^0 and k_{-3}^0 are second-order rate constants. From the perspective of a single enzyme molecule, the reaction is unimolecular and cyclic.

probabilities [20]. Furthermore, we shall discuss the classic Haldane equality in the light of the NESS as well as an unexpected generalization of this equality. The generalized Haldane equation is intimately related to the fluctuation theorems [21].

Next, we shall give three concrete examples of the NESS theory applied to single-molecule enzymology. It is widely believed in molecular biology that biochemical function of a molecule is derived from its structure. While this is certainly true in a general sense, we shall explicitly show how function(s) of a molecule can change depending on the NESS in which the molecular system is situated. The three examples we shall study are (1) a same enzyme modifier switches between being an activator and an inhibitor of an enzyme [22]; (2) how dynamic cooperativity gives rise to an enzyme response that is shaper than MM; and (3) kinetic proofreading in which the specificity between an enzyme–ligands association may not be determined by the equilibrium affinity [23,24]. All these examples together illustrate the importance of non-structural based molecular regulations in the NESS. Specifically, we shall show that all these phenomena will disappear in chemical equilibrium; thus they depend critically upon nonequilibrium kinetic processes rather than merely the static structural properties of macromolecules.

2.1. Cycle fluxes in a nonequilibrium steady-state enzyme

We start by considering a three-step mechanism of an enzymatic reaction in which the conversion of a substrate S into product P in the catalytic site of the enzyme [25,20]

$$E + S \underset{k_{-1}}{\overset{k_1^0}{\rightleftharpoons}} ES \underset{k_{-2}}{\overset{k_2}{\rightleftharpoons}} EP \underset{k_{-3}^0}{\overset{k_3}{\rightleftharpoons}} E + P. \tag{1}$$

If there is only one enzyme molecule, then from the enzyme perspective, the kinetics are stochastic and cyclic, as shown in Fig. 1, with the pseudo-first-order rate constants $k_1 = k_1^0 c_S$ and $k_{-3} = k_{-3}^0 c_P$ where c_S and c_P are the sustained concentrations of substrate S and product P in the steady state.

At the chemical equilibrium, the concentrations of S and P satisfy $c_P/c_S = k_1^0 k_2 k_3 / \left(k_{-1} k_{-2} k_{-3}^0\right)$, i.e.

$$\frac{k_1 k_2 k_3}{k_{-1} k_{-2} k_{-3}} = 1.$$

This is known as the "thermodynamic box" in elementary chemistry, also called detailed balance. However, if the c_S and c_P are maintained at constant levels that are not at chemical equilibrium, as metabolite concentrations are in living cells, the enzyme reaction is in an open system that approaches a NESS. This is the scenario of most enzyme kinetics in a living, homeostatic cell.

In this case,

$$\frac{k_1 k_2 k_3}{k_{-1} k_{-2} k_{-3}} = \gamma \neq 1, \tag{2}$$

and in fact $\Delta\mu = k_B T \ln \gamma$ is the well known chemical potential difference between P and S, independent of the enzyme.

From the perspective of single enzyme molecule, the rate equation for the probabilities of the states follow a master equation

$$\begin{aligned}
\frac{dP_E(t)}{dt} &= -(k_1 + k_{-3})P_E(t) + k_{-1}P_{ES}(t) + k_3 P_{EP}(t),\\
\frac{dP_{ES}(t)}{dt} &= k_1 P_E(t) - (k_{-1} + k_2)P_{ES}(t) + k_{-2}P_{EP}(t),\\
\frac{dP_{EP}(t)}{dt} &= k_{-3}P_E(t) + k_2 P_{ES}(t) - (k_{-2} + k_3)P_{EP}(t).
\end{aligned} \tag{3}$$

The steady-state probabilities for states E, ES and EP are easily computed from setting the time derivative to zero and noting that $P_E + P_{ES} + P_{EP} = 1$ for the total probability:

$$P_E^{ss} = \frac{k_2k_3 + k_{-1}k_3 + k_{-1}k_{-2}}{\mathcal{D}},$$
$$P_{ES}^{ss} = \frac{k_1k_3 + k_{-2}k_{-3} + k_1k_{-2}}{\mathcal{D}},$$
$$P_{EP}^{ss} = \frac{k_1k_2 + k_2k_{-3} + k_{-1}k_{-3}}{\mathcal{D}},$$

in which the denominator

$$\mathcal{D} = k_1k_2 + k_2k_3 + k_3k_1 + k_{-1}k_{-3} + k_{-2}k_{-3} + k_{-1}k_{-2} + k_1k_{-2} + k_2k_{-3} + k_3k_{-1}.$$

Then, the clockwise steady-state cycle flux in Fig. 1, which is precisely the enzyme turnover rate of $S \to P$ in the reaction scheme (1), $J^{ss} = P_E^{ss}k_1 - P_{ES}^{ss}k_{-1} = P_{ES}^{ss}k_2 - P_{EP}^{ss}k_{-2} = P_{EP}^{ss}k_3 - P_E^{ss}k_{-3}$, which follows

$$J^{ss} = \frac{k_1k_2k_3 - k_{-1}k_{-2}k_{-3}}{\mathcal{D}} = J_+^{ss} - J_-^{ss}, \tag{4}$$

where

$$J_+^{ss} = \frac{k_1k_2k_3}{\mathcal{D}}, \qquad J_-^{ss} = \frac{k_{-1}k_{-2}k_{-3}}{\mathcal{D}}, \tag{5}$$

are the forward and backward cycle fluxes, respectively.

The net cycle flux is just the Michaelis–Menten steady-state flux of Fig. 1, i.e.

$$v = \frac{V_S\frac{c_S}{K_{mS}} - V_P\frac{c_P}{K_{mP}}}{1 + \frac{c_S}{K_{mS}} + \frac{c_P}{K_{mP}}},$$

where maximal velocities

$$V_S = \frac{k_2k_3}{k_{-2} + k_2 + k_3}, \qquad V_P = \frac{k_{-1}k_{-2}}{k_{-2} + k_2 + k_{-1}}, \tag{6}$$

and Michaelis constants

$$K_{mS} = \frac{k_{-1}k_{-2} + k_{-1}k_3 + k_2k_3}{k_1^0(k_{-2} + k_2 + k_3)}, \qquad K_{mP} = \frac{k_{-1}k_{-2} + k_{-1}k_3 + k_2k_3}{(k_{-2} + k_2 + k_{-1})k_{-3}^0}. \tag{7}$$

In addition, J_+^{ss} and J_-^{ss} are the averaged numbers of the forward and backward cycles per time respectively due to ergodic theory [20,26], i.e.

$$J^{ss} = \lim_{t\to\infty}\frac{1}{t}\nu(t), \qquad J_+^{ss} = \lim_{t\to\infty}\frac{1}{t}\nu_+(t), \qquad J_-^{ss} = \lim_{t\to\infty}\frac{1}{t}\nu_-(t), \tag{8}$$

where $\nu_+(t)$ and $\nu_-(t)$ are the number of occurrences of forward and backward cycles up to time t, and $\nu(t) = \nu_+(t) - \nu_-(t)$.

Before closing this section, it is important to point out that the quantity γ can be approximated by $\nu_+(t)/\nu_-(t)$ in single-molecule experiment when the time t is large enough, due to the fact that $\gamma = J_+^{ss}/J_-^{ss}$. One also has $J_+^{ss} = J_-^{ss}$, i.e. $\gamma = 1$, if and only if the enzymatic reaction is at chemical equilibrium.

2.1.1. Mean waiting cycle times

In single-molecule enzyme kinetic studies, the most salient feature of either the substrate turnover time courses or the enzyme cyclic trajectories is that they are stochastic. The stochasticity, however, is exhibited in the time needed "waiting" for a chemical reaction to occur via "fluctuating" diffusion encounter and thermal activation. The time needed for actual atomic and molecular motion that accomplishes a chemical reaction is often on the order of subpicosecond which is considered instantaneous in enzyme kinetics in aqueous solution. Therefore, in a single-molecule experiment, the observed state as function of time corresponds to the "stochastic waiting time" for a reaction. Once having a statistical time course data in hand, the most straightforward analysis of the trajectories is clearly the two distributions of the on-time and off-time. Therefore in our theoretical model, we shall first define the waiting cycle times and then calculate their means, variances, and ultimately distributions.

Starting from the free enzyme state E, three kinds of waiting cycle times can be defined: Let T represents the waiting time for the occurrence of a forward or a backward cycle, T_+ represents the waiting time for only the occurrence of a forward cycle, and T_- represents the waiting time for only the occurrence of a backward cycle respectively. Obviously, as three random variables, T is just the smaller one of T_+ and T_-.

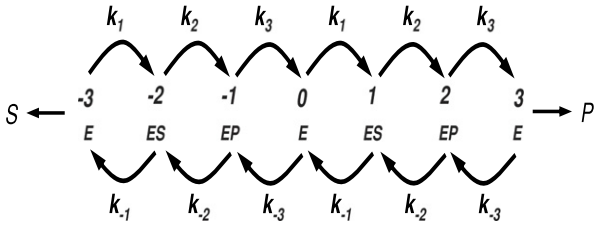

Fig. 2. The kinetic scheme for computing the waiting cycle times T, T_+ and T_-. In order to distinguish the forward and backward cycles, Fig. 1 is transformed into a one-dimensional random walk.

The problem of computing the mean waiting time $\langle T\rangle$ is in fact the same as in the mean first-passage-time (MFPT) problem (Fig. 2) for random walk. This is a perfect application of this classical problem of probability in single-enzyme kinetics.

Let τ_i be the mean time first hitting the state 3 or -3 in Fig. 2, starting from the state i. Obviously, $\langle T\rangle = \tau_0$ and $\tau_3 = \tau_{-3} = 0$.

Then we need to derive the equations for $\{\tau_i\}$. Starting from the state i, it will first wait for an exponential time averaged $\frac{1}{q_{i,i-1}+q_{i,i+1}}$ where q_{ij} is just the reaction constant from state i to state j, then jump to either state $i-1$ or state $i+1$ according to the ratio of their reaction constants. Hence τ_i would be the summation of $\frac{1}{q_{i,i-1}+q_{i,i+1}}$ and the probability weighted mean first hitting time starting from $i-1$ or $i+1$.

Hence τ_i satisfies the following equations with boundary $\langle T\rangle = \tau_0$ and $\tau_3 = \tau_{-3} = 0$:

$$\begin{aligned}
\tau_{-2} &= \frac{1}{k_{-1}+k_2} + \frac{k_{-1}}{k_{-1}+k_2}\times 0 + \frac{k_2}{k_{-1}+k_2}\tau_{-1},\\
\tau_{-1} &= \frac{1}{k_{-2}+k_3} + \frac{k_{-2}}{k_{-2}+k_3}\tau_{-2} + \frac{k_3}{k_{-2}+k_3}\tau_0,\\
\tau_0 &= \frac{1}{k_{-3}+k_1} + \frac{k_{-3}}{k_{-3}+k_1}\tau_{-1} + \frac{k_1}{k_{-3}+k_1}\tau_1,\\
\tau_1 &= \frac{1}{k_{-1}+k_2} + \frac{k_{-1}}{k_{-1}+k_2}\tau_0 + \frac{k_2}{k_{-1}+k_2}\tau_2,\\
\tau_2 &= \frac{1}{k_{-2}+k_3} + \frac{k_{-2}}{k_{-2}+k_3}\tau_1 + \frac{k_3}{k_{-2}+k_3}\times 0.
\end{aligned} \tag{9}$$

Through a simple calculation, one can obtain that

$$\langle T\rangle = \frac{1}{J_+^{ss}+J_-^{ss}}, \tag{10}$$

where J_+^{ss} and J_-^{ss} are given in Eq. (5). Similarly, another mean waiting cycle time $\langle T_+\rangle$, which is the mean time to complete the forward cycle in Fig. 1 whether before or after completing cycling in the opposite direction, can be obtained as the solutions of equations identical to Eq. (9), but with different boundary conditions. Let τ_{i+} be the mean time first hitting the state 3, whether before or after the time hitting the state -3 in Fig. 2, starting from the state i. Obviously, $\langle T_+\rangle = \tau_{0+}$, $\tau_{3+} = 0$ and $\tau_{-3+} = \tau_{0+}$.

Then

$$\langle T_+\rangle = \frac{1}{J_+^{ss}},$$

where J_+^{ss} is given in Eq. (5). Almost with the same derivation one can compute the $\langle T_-\rangle$, which is the mean time to complete the backward cycle in Fig. 1, whether before or after complete cycling in the opposite direction. It immediately follows

$$\langle T_-\rangle = \frac{1}{J_-^{ss}},$$

where J_-^{ss} is given in Eq. (5).

In fact, one can obtain the expression for $\langle T_-\rangle$ (Eq. (5)) directly based on the expression for $\langle T_+\rangle$ (Eq. (5)) according to the symmetry of the random walk in Fig. 2: $(k_1, k_{-1}, k_2, k_{-2}, k_3, k_{-3}) \to (k_{-3}, k_3, k_{-2}, k_2, k_{-1}, k_1)$.

We see that $\langle T_+\rangle = \langle T_-\rangle$ if and only if this system is at chemical equilibrium, because of $\gamma = \langle T_-\rangle/\langle T_+\rangle$. As a consequence, γ can also be measured by the ratio of averaged forward and backward waiting cycle times up to time t in the single-molecule experiment, which is different from its previous measurement $\gamma = \frac{\nu_+(t)}{\nu_-(t)}$. Nevertheless, as indicated in Eq. (8), by applying the elementary renewal theorem, the two methods are asymptotically the same because $\langle T_+\rangle \approx t/\nu_+(t)$ and $\langle T_-\rangle \approx t/\nu_-(t)$ when t is large.

2.1.2. Stepping probabilities

The stepping frequencies $f^+(t)$ and $f^-(t)$ up to time t are just the fractions of $\nu_+(t)$ and $\nu_-(t)$, representing the weights of the forward and backward cycles respectively from the statistical point of view in experiments, i.e.

$$f^+(t) = \frac{\nu_+(t)}{\nu_+(t)+\nu_-(t)}, \qquad f^-(t) = \frac{\nu_-(t)}{\nu_+(t)+\nu_-(t)}.$$

According to Eq. (8), one can get the eventual stepping probability

$$p^+ \overset{\text{def}}{=} \lim_{t\to\infty} f^+(t) = \frac{J_+^{ss}}{J_+^{ss}+J_-^{ss}} = \frac{k_1k_2k_3}{k_1k_2k_3+k_{-1}k_{-2}k_{-3}}, \tag{11a}$$

$$p^- \overset{\text{def}}{=} \lim_{t\to\infty} f^-(t) = \frac{J_-^{ss}}{J_+^{ss}+J_-^{ss}} = \frac{k_{-1}k_{-2}k_{-3}}{k_1k_2k_3+k_{-1}k_{-2}k_{-3}}. \tag{11b}$$

It is necessary to point out that the stepping frequencies $f^+(t)$ and $f^-(t)$ are random variables depending on the trajectories, while their fluctuations tend to vanish when t tends to infinity. Hence the eventual stepping probability p^+ and p^- are independent of the trajectories due to the ergodicity.

Interestingly, the forward stepping probability can also be defined as $p^+ \overset{\text{def}}{=} \Pr_{\{E\}}\{T_+ < T_-\}$, which means the probability that the enzyme first completes a forward cycle, starting from the initial free enzyme state E, before a backward cycle. Similarly, the backward stepping probability can be defined as $p^- \overset{\text{def}}{=} \Pr_{\{E\}}\{T_- < T_+\}$.

This equivalence can also be seen explicitly through translating this problem to the corresponding random walk in Fig. 2. Let p_{i+} be the probability of hitting the state 3 before -3 in Fig. 2, starting from the state i. Obviously, $p_{3+} = 1$ and $p_{-3+} = 0$.

Again applying the strong Markov property of Markov chains as what we have done in the previous section, $\{p_{i+}\}$ satisfies the following equations

$$\begin{aligned}
p_{-2+} &= \frac{k_{-1}}{k_{-1}+k_2}\times 0 + \frac{k_2}{k_{-1}+k_2}p_{-1+},\\
p_{-1+} &= \frac{k_{-2}}{k_{-2}+k_3}p_{-2+} + \frac{k_3}{k_{-2}+k_3}p_{0+},\\
p_{0+} &= \frac{k_{-3}}{k_{-3}+k_1}p_{-1+} + \frac{k_1}{k_{-3}+k_1}p_{1+},\\
p_{1+} &= \frac{k_{-1}}{k_{-1}+k_2}p_{0+} + \frac{k_2}{k_{-1}+k_2}p_{2+},\\
p_{2+} &= \frac{k_{-2}}{k_{-2}+k_3}p_{1+} + \frac{k_3}{k_{-2}+k_3}\times 1.
\end{aligned}$$

Through a similar calculation, one can obtain that

$$p^+ = \Pr_{\{E\}}\{T_+ < T_-\} = p_{0+} = \frac{k_1k_2k_3}{k_1k_2k_3+k_{-1}k_{-2}k_{-3}},$$

and

$$p^- = \Pr_{\{E\}}\{T_+ > T_-\} = 1 - \Pr_{\{E\}}\{T_+ < T_-\} = \frac{k_{-1}k_{-2}k_{-3}}{k_1k_2k_3+k_{-1}k_{-2}k_{-3}}.$$

Consequently,

$$p^+ = \frac{J_+^{ss}}{J_+^{ss}+J_-^{ss}} = \frac{\langle T\rangle}{\langle T_+\rangle}, \qquad p^- = \frac{J_-^{ss}}{J_+^{ss}+J_-^{ss}} = \frac{\langle T\rangle}{\langle T_-\rangle},$$

and chemical potential difference

$$\Delta\mu = k_BT\log\gamma = k_BT\log\frac{p^+}{p^-} = k_BT\log\frac{J_+^{ss}}{J_-^{ss}} = k_BT\log\frac{\langle T_-\rangle}{\langle T_+\rangle}, \tag{12}$$

which follows $p^+ = p^-$ if and only if the enzyme reaction is at chemical equilibrium.

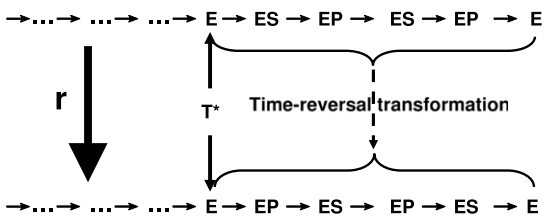

Fig. 3. An illustrative example of the "quasi-time-reversal" map. T^* is the *last time* when it leaves the state $\{E\}$ before finishing a forward cycle $E \to ES \to EP \to E$, then one maps the real time-reversal trajectory of ω with respect to the time interval $[T^*, T_+]$ to $r\omega$. See text for details.

2.1.3. Haldane equality and its generalization

The Haldane equality in enzyme kinetics is between the forward Michaelis constant K_M, maximum velocity $V_{\max}$, and the backward ones. Using the results in Eqs. (6) and (7), we see that

$$\frac{V_S/K_{mS}}{V_P/K_{mP}} = \frac{k_1^0 k_2 k_3}{k_{-1}k_{-2}k_{-3}^0}. \tag{13}$$

The right-hand-side is independent of the enzyme. In other words, $(V_S/K_{mS})c_S = \gamma(V_P/K_{mP})c_P$. The Haldane equality in Eq. (13), thus, is simply an alternative expression for the Eq. (12): $\left(1 + \frac{c_S}{K_{mS}} + \frac{c_P}{K_{mP}}\right) K_{mS}/(V_S c_S) = \langle T_+ \rangle$ and $\left(1 + \frac{c_S}{K_{mS}} + \frac{c_P}{K_{mP}}\right) K_{mP}/(V_P c_P) = \langle T_- \rangle$!

An interesting observation from single-molecule enzyme kinetics generalized Haldane equality: not only the mean values of cycles times T_- and γT_+ the same, their entire probability distributions are identical, both are the same as that of T. In fact, waiting cycle time T is *independent* of whether the enzyme E completes a forward cycle or a backward cycle, although the probability of these two cycles might be rather different (i.e., $\gamma \neq 1$).

We introduce a one-to-one "quasi-time-reversal" mapping r for the trajectory of the simple kinetic in Fig. 1, which belongs to the event $\{T_+ < T_-\}$, mapped to its "quasi-time-reversal" one [20].

For each trajectory $\omega = \{\omega_t : t \geq 0, \omega_0 = \{E\}\}$ belonging to the set $\{T_+ < T_-\}$, let T^* be the *last time* when it leaves the state $\{E\}$ before finishing a forward cycle in the Fig. 1. Then its "quasi-time-reversal" one $r\omega = \{(r\omega)_t : t \geq 0\}$ is defined as follows:

(i) when the time t is before or equal to T^*, then one just copy ω to $r\omega$, i.e. $(r\omega)_t = \omega_t$;
(ii) when the time t is between T^* and T_+, then one maps the real time-reversal trajectory of ω with respect to the time interval $[T^*, T_+]$ to $r\omega$, i.e. $(r\omega)_t = \omega_{T^*+T_+-t}$;
(iii) when the time t is greater than T_+, then one can also simply copy ω to $r\omega$ as what we have done in (i).

See Fig. 3 for an illustrative example. As was pointed out in the figure's caption, T^* is denoted to be the *last time* when it leaves the state $\{E\}$ before finishing a forward cycle $E \to ES \to EP \to E$. Then *the ratio* of the probability density of the above trajectory with respect to its "quasi-time-reversal" one below is

$$\gamma = \frac{k_1 k_2 k_{-2} k_2 k_3}{k_{-3} k_{-2} k_2 k_{-2} k_{-1}} = \frac{k_1 k_2 k_3}{k_{-1} k_{-2} k_{-3}}.$$

Now it is indispensable to explain why we construct the above mapping like this.

(1) The number of the steps $E \to ES$ in the original trajectory ω belonging to $\{T_+ < T_-\}$ is one more than that in its "quasi-time-reversal" corresponding trajectory $r\omega$ belonging to $\{T_+ > T_-\}$, while the number of the steps $ES \to E$ in ω is one less than that in $r\omega$;
Similarly,
(2) The number of the steps $ES \to EP$ in the trajectory ω is one more than that in $r\omega$, while the number of the steps $EP \to ES$ in the trajectory ω is one less than that in $r\omega$;
(3) The number of the steps $EP \to E$ in the trajectory ω is one more than that in $r\omega$, while the number of the steps $E \to EP$ in the trajectory ω is one less than that in $r\omega$; and more important
(4) The dwell time upon each state of the trajectory ω and its "quasi-time-reversal" corresponding one $r\omega$ is mapped quite well such that the difference between ω and $r\omega$ are only exhibited upon their sequences of states.

Consequently, the most important observation is that *the ratio* of the probability density of each trajectory ω in $\{T_+ < T_-\}$ with respect to its "quasi-time-reversal" trajectory $r\omega$ in $\{T_+ > T_-\}$ is invariable, which is, surprisingly, always equal to the constant $\gamma = k_1 k_2 k_3/(k_{-1}k_{-2}k_{-3})$.

Furthermore, the map r is a one-to-one correspondence between the trajectory sets $\{T_+ < T_-\}$ and $\{T_+ > T_-\}$. More particularly, for each $t \geq 0$, the map r is also actually a one-to-one correspondence between the trajectory sets $\{T_+ = t < T_-\}$ and $\{T_+ > T_- = t\}$.

Therefore, for each $t \geq 0$,

$$\Pr_{\{E\}}\{T_+ = t, T_+ < T_-\} = \gamma \Pr_{\{E\}}\{T_- = t, T_- < T_+\},$$

and

$$p^+ = \Pr_{\{E\}}\{T_+ < T_-\} = \gamma \Pr_{\{E\}}\{T_- < T_+\} = \gamma p^-,$$

which has already been proved in the previous section, Eq. (12).

Denote the conditional probability density of T_+ given that $\{T_+ < T_-\}$ as $\Theta_+(t)dt = \Pr_{\{E\}}\{t \leq T_+ < t + dt | T_+ < T_-\}$, and the conditional probability density of T_- given that $\{T_- < T_+\}$ as $\Theta_-(t)dt = \Pr_{\{E\}}\{t \leq T_- < t + dt | T_- < T_+\}$. Hence,

$$\begin{aligned}
\Theta_+(t)dt &= \Pr_{\{E\}}\{t \leq T_+ < t + dt | T_+ < T_-\} \\
&= \frac{\Pr_{\{E\}}\{t \leq T_+ < t + dt, T_+ < T_-\}}{\Pr_{\{E\}}\{T_+ < T_-\}} \\
&= \frac{\gamma \Pr_{\{E\}}\{t \leq T_- < t + dt, T_- < T_+\}}{\gamma \Pr_{\{E\}}\{T_- < T_+\}} \\
&= \Pr_{\{E\}}\{t \leq T_- < t + dt | T_- < T_+\} = \Theta_-(t)dt, \quad \forall t.
\end{aligned}$$

And also denote the probability density of T as $\Theta(t)dt = \Pr_{\{E\}}\{t \leq T < t + dt\}$, so

$$\Theta(t) = \Theta_+(t)p^+ + \Theta_-(t)p^- = \Theta_+(t) = \Theta_-(t).$$

It consequently follows a very important corollary that the distribution of waiting cycle time T is *independent* of whether the enzyme E completes a forward cycle or a backward cycle, although the probability of these two cycles might be rather different, i.e.

$$\begin{aligned}
P_{\{E\}}(t \leq T < t + dt, T_+ < T_-) &= P(t \leq T_+ < t + dt, T_+ < T_-) \\
&= \Theta_+(t)dtp^+ = \Theta(t)dtp^+,
\end{aligned} \tag{14}$$

and

$$\begin{aligned}
P_{\{E\}}(t \leq T < t + dt, T_+ > T_-) &= P(t \leq T_- < t + dt, T_+ < T_-) \\
&= \Theta_-(t)dtp^- = \Theta(t)dtp^-.
\end{aligned} \tag{15}$$

Furthermore, we have

$$\begin{aligned}
\langle T_+, T_+ < T_- \rangle &= p^+ \langle T \rangle, \\
\langle T_-, T_- < T_+ \rangle &= p^- \langle T \rangle,
\end{aligned}$$

and

$$\langle T_+ | T_+ < T_- \rangle = \langle T_- | T_- < T_+ \rangle = \langle T \rangle,$$

which means even in the far from equilibrium case ($\gamma \gg 1$), the dwell times for each forward cycle and that for each backward cycle are identical although their frequencies may be very different ($p^+ \gg p^-$). Such an important equality has been discovered in the context of motor proteins, either experimental or theoretical [27,28].

Now as a closing of this section, we shall present an interesting corollary about the entropy production rate e_p. See Section 2.3 of Part I. We have already shown that

$$e_p = (J_+^{ss} - J_-^{ss}) \log \gamma, \tag{16}$$

where $\log \gamma = \log(J_+^{ss}/J_-^{ss})$ is the entropy production of the single cycle $E \to ES \to EP \to E$, and $J_+^{ss} - J_-^{ss}$ is the net cycle flux: number of cycles per time.

Applying Eq. (16) to waiting cycle times, e_p can be expressed as

$$\begin{aligned}
e_p &= \left(\frac{1}{\langle T_+ \rangle} - \frac{1}{\langle T_- \rangle} \right) \log \gamma \\
&= \left(\frac{p^+}{\langle T \rangle} - \frac{p^-}{\langle T \rangle} \right) \log \gamma \\
&= (p^+ - p^-) \times \text{avepr},
\end{aligned} \tag{17}$$

where

$$\text{avepr} = \frac{1}{\langle T\rangle}\log\gamma = \frac{1}{\langle T\rangle}\log\frac{J_+^{ss}}{J_-^{ss}} = \frac{1}{\langle T\rangle}\log\frac{\langle T_-\rangle}{\langle T_+\rangle} = \frac{1}{\langle T\rangle}\log\frac{p^+}{p^-}$$

is regarded as the time-averaged entropy production rate of the cycle $E \to ES \to EP \to E$.

Finally, recalling that J_+^{ss} and J_-^{ss} can be approximated by $\nu_+(t)$ and $\nu_-(t)$ respectively, it should be emphasized that this entropy production rate can also be measured by $(\nu_+(t) - \nu_-(t))\log(\nu_+(t)/\nu_-(t))$ when the time t is large in a single-molecule experiment [29].

2.1.4. Fluctuation theorems

There is a deep connection between the generalized Haldane equation in the previous section and the fluctuation theorems widely studied in statistical physics in recent years [30–32,21,33]. In this section we give a brief account of two fluctuation theorems: one for the stochastic number of substrate cycle $\nu(t)$ and one for the fluctuating chemical work done for sustaining the NESS $W(t) = \nu(t)\Delta\mu/k_BT = \nu(t)\log\gamma$.

Regarding the probability distribution of the non-stationary process $\nu(t) = \nu_+(t) - \nu_-(t)$, one has

$$\begin{aligned}\Pr\{\nu(t) = k\} &= \sum_{n-r=k}\Pr\{\nu_+(t) = n,\ \nu_-(t) = r\}\\ &= \sum_{n-r=k}^{\infty}\Pr\{\nu_+(t) + \nu_-(t) = n + r\}C_{n+r}^{n}(p^+)^n(p^-)^r,\end{aligned}$$

and

$$\Pr\{\nu(t) = -k\} = \sum_{n-r=k}^{\infty}\Pr\{\nu_+(t) + \nu_-(t) = n + r\}C_{n+r}^{r}(p^+)^r(p^-)^n.$$

Note that p^+ and p^- are the stepping probabilities, and $C_{n+r}^{r} = C_{n+r}^{n} = (n+r)!/(n!\cdot r!)$ is the standard combinatorial factor.

Since $p^+/p^- = \gamma$, we have

$$\frac{\Pr\{\nu(t) = k\}}{\Pr\{\nu(t) = -k\}} = \gamma^k,$$

which is called a transient fluctuation theorem for $\nu(t)$.

Therefore,

$$\begin{aligned}\langle e^{-\lambda\nu(t)}\rangle &= \sum_{k=-\infty}^{\infty}\Pr\{\nu(t) = k\}e^{-k\lambda} = \sum_{k=-\infty}^{\infty}\Pr\{\nu(t) = -k\}e^{-k(\lambda-\log\gamma)}\\ &= \langle e^{-(\log\gamma-\lambda)\nu(t)}\rangle,\end{aligned} \tag{18}$$

which is just the fluctuation theorem in the form of Kurchan–Lebowitz–Spohn-type symmetry. If one let $\lambda = \log\gamma$, then the special case of Kawasaki equality arises

$$\langle e^{-W(t)}\rangle = 1. \tag{19}$$

Eq. (19) is also in the form of the so-called Hatano–Sasa equality [34].

In the previous section, most of the results are obtained through solving a system of linear equations similar to Eq. (9) (Kolmogorov backward form of a master equations). The results can be extended to the n-step cycle [20], according the elementary renewal theorem in probability theory and general circulation theory of Markov chains presented in Section 2.3 of Part I. The key method, however, is still the same "quasi-time-reversal" mapping r introduced in the previous section.

2.2. Modifier activation–inhibition switching in enzyme kinetics

Reversible modifiers of an enzyme is a ligand that can form a dynamic complex with the enzyme and can cause its catalytic properties to change. Reversible enzyme modifiers play a crucial role in both regulations of metabolic pathways inside a cell and in the studies of enzymatic catalysis and functions. Moreover, they have found wide applications in pharmacology and toxicology, as well as in industry and in agriculture. A modifier is called an activator or an inhibitor according to its ability to increase or to decrease the catalytic rate of an enzyme.

In molecular biology, an activator or an inhibitor of an enzyme is widely assumed to be an attribute of the modifying substance, determined by its molecular structure. In this section, we shall show how a same ligand can be both, depending upon the *context* of the biochemical reaction system: the NESS. This idea was first discussed in [35]. Recently, [22,36] have independently carried extensive analysis of this phenomenon.

Though it is a classic problem [37], it was only fully understood recently [22] through the theory of NESS. We start our discussion with a simple example.

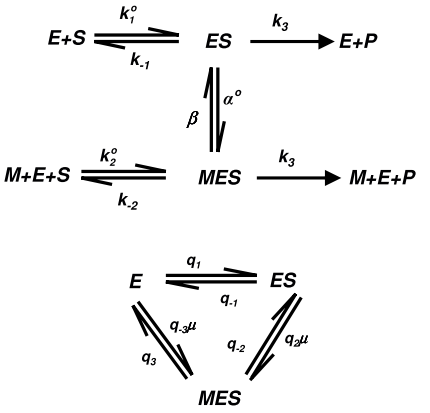

Fig. 4. In the upper enzyme reaction system with a modifier, M, k_1^0 and α^0 are second-order rate constants, and k_2^0 is a third-order rate constant. In the absence of the modifier, $u = 0$, the steady state velocity of the enzymatic reaction is the Michaelis–Menten hyperbolic $\frac{k_1 k_3[S]}{k_1[S]+k_{-1}+k_3}$. In the lower tri-state single enzyme representation for the system: $q_1 = k_1^0[S]$, $q_{-1} = k_{-1} + k_3$, $q_2 = \alpha^0$. $q_{-2} = \beta$, $q_3 = k_{-2} + k_3$, $q_{-3} = k_2^0[S]$, and u is the concentration of the modifier, $[M]$.

2.2.1. Case study of a simple example

Consider a simple enzyme catalyzed reaction that is regulated by a modifier M: There are parallel catalysis pathways with and without the modifier, as shown in the upper panel of Fig. 4. Notice that the system in Fig. 4 contains irreversible steps, hence states ES and E would never reach an equilibrium due to the presence of a flux. However, a NESS among states E, ES and MES can be reached in a single enzyme just as in the standard Michaelis–Menten kinetics which also contains an irreversible step. The absence of backward steps $E + P \to EP$ and $M + E + P \to MEP$ is achieved if we assume the sustained concentration of product P vanishes, i.e. $[P] = 0$. The same situation applies for all irreversible enzyme kinetics.

A molecule M is called an activator (inhibitor) of an enzyme if the enzyme catalyzed reaction velocity is greater (smaller) in the presence of the M. We shall show that, however, in certain kinetic systems a same molecule can act as either an activator or an inhibitor depending upon its concentration $[M]$. There can be a switching from one to another with changing $[M]$. We call this phenomenon kinetic based activation–inhibition switching.

From the standpoint of a single enzyme, there are two types of kinetic cycles in Fig. 4: one substrate binding cycle $M+E+S \rightleftharpoons M+ES \rightleftharpoons MES \rightleftharpoons M+E+S$, and two catalytic cycles $E+S \rightleftharpoons ES \to E+P$, $M+E+S \rightleftharpoons MES \to M+E+P$. The former should obey the detailed balance condition ($k_2^0 \beta k_{-1} = k_1^0 \alpha^0 k_{-2}$) while the latter does not since there is a continuous $S \to P$ turnover.

Since the rate constants for both $ES \to E + S$ and $MES \to M + E + S$ are the same k_3, the rate of catalytic reaction $v = k_3(p_{ES} + p_{MES})$. In order to show the activation–inhibition switching is a NESS phenomenon, we shall first consider the "control" case of E, ES and MES being at equilibrium with each other, when

$$[ES]^{eq} = \frac{k_1^0[E]^{eq}[S]^{eq}}{k_1} \quad \text{and} \quad [MES]^{eq} = \frac{\alpha^0[M]^{eq}[ES]^{eq}}{\beta}.$$

Then the corresponding equilibrium turnover rate

$$v^{eq} = k_3 \left(\frac{\frac{k_1^0[S]^{eq}}{k_{-1}} + \frac{k_1^0[S]^{eq}\alpha^0[M]^{eq}}{k_{-1}\beta}}{1 + \frac{k_1^0[S]^{eq}}{k_{-1}} + \frac{k_1^0[S]^{eq}\alpha^0[M]^{eq}}{k_{-1}\beta}} \right). \tag{20}$$

We see that it always increases with $[M]^{eq}$. Hence the modifier in this model is an activator, never being an inhibitor in equilibrium state.

The NESS of the kinetic system in the upper panel of Fig. 4, with irreversible steps, can be readily solved. This involves a mathematical "trick" that combines rate constants k_3 with k_{-1} and k_{-2}, as shown in the lower panel.[1] Hence the total enzyme-substrate complex (TES)

$$p_{\mathrm{TES}}^{ss}(u) = (p_{ES} + p_{MES})^{ss} = \frac{A + Bu + Cu^2}{D + Eu + Fu^2}. \tag{21}$$

[1] When combining steps like this, it is very important to make an distinction between the mathematical trick and the physical reality: for some particular values of k's, the resulting tri-state Markov chain in the lower panel of Fig. 4 could have $q_1 q_2 q_3 = q_{-1} q_{-2} q_{-3}$. That *does not* mean the physical problem is an equilibrium; rather it is because the mathematical simplification causes some confusion. In order to articulate this distinction, Vellela and Qian [38] have introduced the notion of *chemical detailed balance* and *mathematical detailed balance*. A Markov chain with the latter could still be a useful mathematical model for a nonequilibrium chemical system. However, it can be shown that a mathematical model for the former has to be the latter.

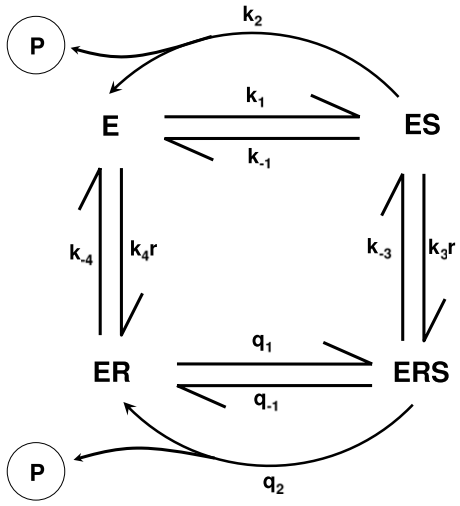

Fig. 5. Kinetic scheme of enzyme reaction with general modifier. The pseudo-first-order rate constants $k_1 = k_1^0 s$, $q_1 = q_1^0 s$. s and r are the substrate concentration and the modifier concentration respectively.

in which u is the concentration of the modifier M,

$$A = q_1 (q_3 + q_{-2}), \qquad B = q_{-2}q_{-3} + q_1 q_2 + q_{-1}q_{-3}, \tag{22a}$$

$$C = q_2 q_{-3}, \qquad D = (q_1 + q_{-1})(q_3 + q_{-2}), \tag{22b}$$

$$E = q_{-2}q_{-3} + q_1 q_2 + q_{-1}q_{-3} + q_2 q_3, \qquad F = q_2 q_{-3}. \tag{22c}$$

We see that

$$p_{\mathrm{TES}}^{ss}(0) = \frac{A}{D} = \frac{k_1}{k_1 + k_{-1}} < p_{\mathrm{TES}}^{ss}(\infty) = \frac{C}{F} = 1.$$

and

$$\left(p_{\mathrm{TES}}^{ss}\right)'(0) = \frac{B}{A} - \frac{E}{D} = \frac{q_{-1}(q_{-2}q_{-3} + q_1 q_2 + q_{-1}q_{-3}) - q_1 q_2 q_3}{q_1(q_3 + q_{-2})(q_1 + q_{-1})}. \tag{23}$$

If $\left(p_{\mathrm{TES}}^{ss}\right)'(0) < 0$, then there is an inhibition to activation switching with increasing $[M]$. One can in fact obtain the critical u_c value (switching point):

$$\frac{A + Bu_c + Cu_c^2}{D + Eu_c + Fu_c^2} = \frac{A}{D}.$$

This yields,

$$u_c = \frac{DC - AF}{AE - DB} = \frac{F}{A}\left(\frac{\frac{C}{F} - \frac{A}{D}}{\frac{E}{D} - \frac{B}{A}}\right) > 0.$$

2.2.2. Modifier with a more general mechanism—an in-depth study

As early as 1953, Botts and Morales [39] have considered a mechanism for a general modifier with reversible binding with a Michaelis–Menten kinetics. The four-state catalytic reaction system shown in Fig. 5 is central to their mechanism. Fig. 5 is also kinetically isomorphic to the fluctuating enzyme model of Witzel–Frieden [40–42]. Many previous works have studied the steady-state as well as transient kinetics of this general modifier mechanism.

Here, we shall discuss the rate of product formation associated with the general modifier mechanism in Fig. 5, in which E, S, R and P stand for the enzyme, the substrate, the regulator (modifier) and the product respectively, and ES, ER and ERS are three complexes, whose meanings are self-evident. k_1^0, q_1^0 are second-order rate constants. This mechanism can produce hyperbolic inhibition or activation, or a combination of the two. All of the simple mechanisms for inhibition and activation (apart from product inhibition) are special cases of this general mechanism [37].

Similar to the previous subsection, the rate for product formation from an enzyme-modifier system at equilibrium is

$$v^{eq}(r) = k_2 p_{ES}^{eq} + q_2 p_{ERS}^{eq} = \frac{k_2 \frac{k_1}{k_{-1}} + q_2 \frac{k_1 k_3 r}{k_{-1}k_{-3}}}{1 + \frac{k_1}{k_{-1}} + \frac{k_1 k_3 r}{k_{-1}k_{-3}} + \frac{k_4 r}{k_{-4}}}, \tag{24}$$

in which $r = [R]$, $k_1 = k_1^0[S]$ and $q_1 = q_1^0[S]$. In the derivation of Eq. (24), we have used the detailed balance in the substrate-binding cycle: $k_1k_3q_{-1}k_{-4} = k_{-1}k_{-3}q_1k_4$. Again, with fixed $[S]^{eq}$, $v^{eq}(r)$ is always monotonic with respect to r.

Moreover, we have

$$v^{eq}(0) = \frac{k_2\frac{k_1}{k_{-1}}}{1+\frac{k_1}{k_{-1}}},$$

and

$$v^{eq}(\infty) = \frac{q_2\frac{k_1k_3}{k_{-1}k_{-3}}}{\frac{k_1k_3}{k_{-1}k_{-3}}+\frac{k_4}{k_{-4}}},$$

hence when $(v^{eq}(\infty) - v^{eq}(0)) > 0$, the modifier acts as an activator, and otherwise as inhibitor. This is true for all value of r. Both $v^{eq}(\infty)$ and $v^{eq}(0)$ could be measured directly and are functions of rate constants ks and qs, which are intrinsic properties of the molecules E, R and their interaction. Hence whether the R is an equilibrium activator or inhibitor is solely determined by the molecular structures as well as the concentration of S.

In a NESS, from a single enzyme perspective, the kinetics described in Fig. 5 can be represented as a Markov chain $\xi(t)$ with the finite discrete state space $\mathcal{S} = \{E, ES, ER, ERS\}$ and the continuous-time parameter t. The rate matrix Q of the transition probability of the Markov chain can be readily written down from Fig. 5:

$$Q = \begin{pmatrix} -(k_1+k_4r) & k_1 & k_4r & 0 \\ k_{-1}+k_2 & -(k_{-1}+k_2+k_3r) & 0 & k_3r \\ k_{-4} & 0 & -(k_{-4}+q_1) & q_1 \\ 0 & k_{-3} & q_{-1}+q_2 & -(q_{-1}+q_2+k_{-3}) \end{pmatrix},$$

where the rows and columns are indexed by $\mathcal{S}$, and r again is the modifier concentration. We will only study the steady state and assume that the concentration s of the substrate and the concentration p of the product are kept constant in some way (in fact $p = 0$ as in the previous section). This assumption implies that the single, irreversible enzyme reaches a NESS in general.

Let $p^{ss} = (p^{ss}_E, p^{ss}_{ES}, p^{ss}_{ER}, p^{ss}_{ERS})$ be the invariant probability distribution of the Markov chain $\xi(t)$. Then in the steady state the rate for product formation is

$$v(r) = k_2p^{ss}_{ES} + q_2p^{ss}_{ERS}.$$

The rate of product formation $v(r)$ is dependent upon the concentration of the modifier, r, via p^{ss}, which is obtained by solving the system of linear equations $p^{ss}Q = 0$. By obtaining the expression of $v(r)$ in terms of r and examining the influence of r on $v(r)$, the kinetics can be analyzed.

We shall not present the mathematical details here but wish only to give a brief summary of the phenomenon. For a comprehensive account please see [22].

Hyperbolic behavior. Under certain conditions, the steady-state velocity of product formation $v(r)$ in a NESS exhibits approximately hyperbolic dependence on r, the concentration of the modifier R. In this case, the modifier behaves in the same way as it does at equilibrium steady state. (Solid line in Fig. 6.)

Bell-shaped behavior. The velocity $v(r)$ in the NESS also could exhibit a bell-shaped dependence on $[R]$. In this case the quantity Δv is always positive or negative according to whether $v(\infty)$ is greater or smaller than $v(0)$. Although both the hyperbolic-behaved and bell-shaped-behaved modifiers are overall activators or inhibitors for all possible values of the modifier concentration $[R]$, the bell-shaped-behaved modifier would make the enzyme activity exceed its limit value of saturated rate. (Dashed line in Fig. 6.)

Switching behavior. More interestingly, in this case, the quantity Δv may change the sign somewhere in the range of modifier concentration. The role played by the modifier will convert from an activator to an inhibitor or vice versa. Therefore at the NESS, the effect of activation or inhibition should not be viewed as an intrinsic property of the modifier. It depends on the concentrations of the modifier $[R]$. (Dotted line in Fig. 6.)

2.3. Fluctuating enzymes and dynamic cooperativity

Many experimental measurements have shown that most enzymes have a great deal of conformational fluctuations, also called dynamic disorder.[2] One of the surprising consequences of this, when an enzyme operates in a living cellular environment (see below), is that the enzyme catalysis can exhibit positive cooperativity, giving rise to a "sigmoidal dependence" of the product formation rate as a function of the substrate concentration in steady state [40,41,11]. We now study this phenomenon.

[2] Dynamic disorder refers to the behavior that a reaction rate constant fluctuates as a function of time. One of the mechanisms for such phenomenon is that a reactant has fluctuations among multiple conformations, each with a different reaction rate constant.

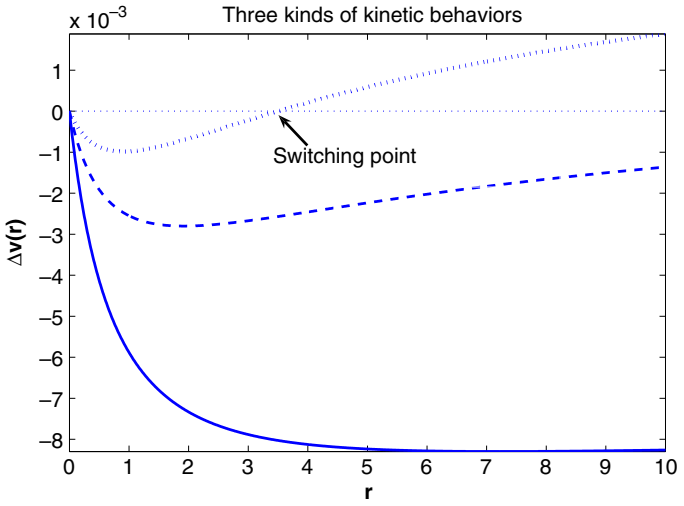

Fig. 6. Three kinds of kinetic behaviors in the general regulation mechanism (Fig. 5). $\Delta v(r) = v(r) - v(0)$. Parameters: $k_1 = 2$; $k_2 = 0.1$; $k_{-1} = 2 - k_2$; $q_1 = 1$; $q_2 = 0.085$ (solid), 0.102 (dashed) and 0.11 (dotted); $q_{-1} = 1 - q_2$; $k_3 = 1$; $k_{-3} = 2$; $k_4 = 2$; $k_{-4} = 1$. Here γ is kept to be 1/4.

2.3.1. Universal Michaelis–Menten equation for enzymes with a single unbound state

We shall consider the waiting cycle time in this case: a free enzyme molecule would wait for an exponential time with mean $\frac{a}{[S]}$; and then be transferred to bounded state. No matter how complex the reaction scheme within bounded states, the initial bounded state would wait for a stochastic time with mean b, and then jump back to the free state, giving rise to either a substrate molecule or a product molecule with probabilities p_1 and $1 - p_1$ respectively. Hence we derive the equation for the mean waiting cycle time $\langle T\rangle$:

$$\langle T\rangle = \frac{a}{[S]} + b + p_1\langle T\rangle,$$

which followed by

$$J = \frac{1}{\langle T\rangle} = \frac{1-p_1}{\frac{a}{[S]} + b} = \frac{(1-p_1)[S]}{b[S] + a}.$$

This is precisely the Michaelis–Menten kinetics.

2.3.2. A simple model for fluctuating enzyme

As we have shown, if there is only one unbound enzyme state E, then no matter how complex the reaction scheme within the ES state is, the Michaelis–Menten kinetics is valid. So we consider the situation of having two unbound enzyme states E_1 and E_2, both can bind the substrate S and to form ES.

For simplicity, we assume that the E_1S and E_2S are essentially the same. So we have the simplest kinetic model for fluctuating enzyme

$$E_1 \underset{k_{-1}}{\overset{k_1}{\rightleftharpoons}} E_2, \qquad E_1 + S \underset{\beta_1}{\overset{\alpha_1}{\rightleftharpoons}} ES, \qquad E_2 + S \underset{\beta_2}{\overset{\alpha_2}{\rightleftharpoons}} ES,$$
$$ES \xrightarrow{\alpha_3} E_1 + P, \qquad ES \xrightarrow{\alpha_4} E_2 + P. \tag{25}$$

Wong and Hanes has put forward a similar model in 1962 [43]. Frieden introduced the concept of hysteretic enzyme as early as 1970 [40], while Ricard and his colleagues have championed the concept of mnemonic enzyme [41]. See [11,42] for two recent account in the light of single-molecule enzymology. As we shall show, while both hysteretic and monomeric enzymes are consequences of slow conformational disorder, they are in fact saying something different: One concept emphasizes transient kinetics and the other relates to a driven NESS.

Similar to the previous section, we assume the sustained $[P]^{ss} = 0$ here, hence an enzyme would reach a nonequilibrium steady state (NESS) with non-zero flux. When an enzyme is in equilibrium with detailed balance, however,

$$\theta(s) = \frac{[ES]}{E_{\text{tot}}} = p_{ES} = \frac{\frac{k_1\alpha_2[S]^{eq}}{k_{-1}\beta_2}}{1 + \frac{k_1}{k_{-1}} + \frac{k_1\alpha_2[S]^{eq}}{k_{-1}\beta_2}},$$

with the thermodynamic constrain $k_1\alpha_2\beta_1 = k_{-1}\alpha_1\beta_2$. This is always hyperbolic.

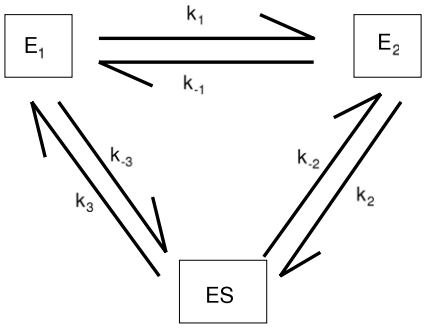

Fig. 7. A tri-state Markov system representing the simplest fluctuating enzyme with two distinctly different unbound states E_1 and E_2, where $k_2 = \alpha_2[S]$, $k_3 = \beta_1 + \alpha_3$, $k_{-2} = \beta_2 + \alpha_4$ and $k_{-3} = \alpha_1[S]$.

In nonequilibrium steady state, from a single-enzyme perspective, we have a tri-state Markov system shown in Fig. 7. We shall assume that the fluctuating rates between E_1 and E_2, k_1 and k_{-1}, are small. Otherwise, if they are fast, then this model is reduced to the simple Michaelis–Menten kinetics with association rate constant $(k_{-1}\alpha_1 + k_1\alpha_2)/(k_{-1} + k_1)$ and dissociation rate constant $\beta_1 + \beta_2$.

Simple calculation gives

$$p_E = \frac{[E]}{E_{\text{tot}}} = \frac{k_2k_3 + k_{-1}k_3 + k_{-1}k_{-2}}{\mathcal{D}},$$
$$p_{E^*} = \frac{[E^*]}{E_{\text{tot}}} = \frac{k_1k_3 + k_{-2}k_{-3} + k_1k_{-2}}{\mathcal{D}},$$

and

$$p_{ES} = \frac{[ES]}{E_{\text{tot}}} = \frac{k_1k_2 + k_2k_{-3} + k_{-1}k_{-3}}{\mathcal{D}},$$

and

$$\mathcal{D} = k_2k_3 + k_{-1}k_3 + k_{-1}k_{-2} + k_1k_3 + k_{-2}k_{-3} + k_1k_{-2} + k_1k_2 + k_2k_{-3} + k_{-1}k_{-3}.$$

Hence

$$\theta(s) = \frac{[ES]}{E_{\text{tot}}} = \frac{ds + cs^2}{a + bs + cs^2}, \tag{26}$$

where $a = k_{-1}k_3 + k_{-1}k_{-2} + k_1k_3 + k_1k_{-2}$, $b = \alpha_2k_3 + k_{-2}\alpha_1 + k_1\alpha_2 + k_{-1}\alpha_1$, $c = \alpha_1\alpha_2$ and $d = k_1\alpha_2 + k_{-1}\alpha_1$.

The steady state velocity of the enzyme catalyzed reaction is $v = (\alpha_3 + \alpha_4)\theta(s)$. It contains terms with $[S]^2$. Then the fluctuating enzyme is possible to have its catalyzed reaction velocity exhibiting a sigmoidal dependence on the substrate concentration s. This is known as dynamic cooperativity, in contrast to the allosteric cooperativity which requires multiple binding sites within an enzyme. This phenomenon is also known as mnemonic behavior. Both dynamic disorder and the breakdown of detailed balance are necessary for a monomeric enzyme to show this interesting behavior in the NESS.

Applying the mathematical method in Section 2.3.3, we obtain $ac - d(b-d)$ in Eq. (26) to be $(k_{-1}k_{-2}\alpha_1 - k_1\alpha_2k_3)(\alpha_2 - \alpha_1)$. Hence positive cooperativity corresponds to $k_1\alpha_2k_3 < k_{-1}k_{-2}\alpha_1$ (Fig. 8) and negative cooperativity corresponds to $k_1\alpha_2k_3 > k_{-1}k_{-2}\alpha_1$ when $\alpha_2 > \alpha_1$. When $\alpha_2 = \alpha_1$, the catalytic capability is the same for both of the two different enzyme conformations, so there will always have a hyperbolic mechanism.

Similar result holds for more general cases (Fig. 9), where

$$\theta(s) = \frac{[ES] + [E^*S]}{E_{\text{tot}}} = \frac{ds + cs^2}{a + bs + cs^2}$$

where

$$a = k_{-1}k_{-2}k_{-3} + k_{-1}k_{-2}k_4 + k_{-1}k_3k_4 + k_1k_{-2}k_{-3} + k_1k_{-2}k_4 + k_1k_3k_4,$$
$$b = k_2k_3k_4 + k_{-2}k_{-3}k_{-4} + k_1k_2k_3 + k_{-1}k_{-2}k_{-4} + k_{-1}k_3k_{-4} + k_1k_2k_{-3} + k_1k_2k_4 + k_{-1}k_{-3}k_{-4},$$
$$c = k_2k_3k_{-4} + k_2k_{-3}k_{-4},$$
$$d = k_1k_2k_3 + k_{-1}k_{-2}k_{-4} + k_{-1}k_3k_{-4} + k_1k_2k_{-3} + k_1k_2k_4 + k_{-1}k_{-3}k_{-4}.$$

Again applying the mathematical method in Section 2.3.3, one obtains that $ac - d(b - d) = (k_{-1}k_{-2}k_{-3}k_{-4} - k_1k_2k_3k_4)(k_2k_{-3} + k_2k_4 + k_2k_3 - k_{-3}k_{-4} - k_{-2}k_{-4} - k_3k_{-4})$. Similar conclusion as in the previous simple model can be reached.

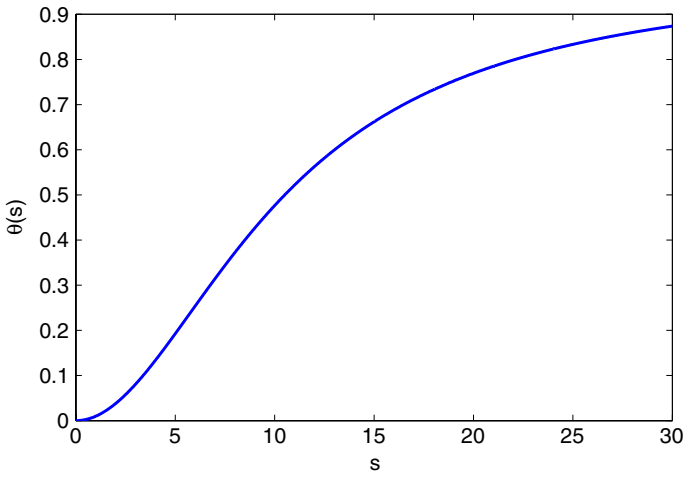

Fig. 8. Positive dynamic cooperativity in the simple model (Fig. 7). Parameters: $k_1 = 0$; $k_{-1} = 1$; $\alpha_1 = 0.01$; $k_{-2} = 100$; $k_3 = 0$; $\alpha_2 = 100$.

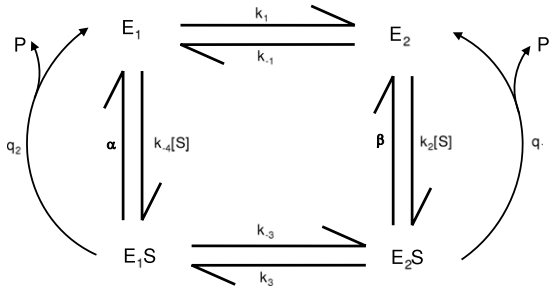

Fig. 9. The canonical four-state model for fluctuating enzyme, where $k_4 = \alpha + q_2$ and $k_{-2} = \beta + q_1$.

2.3.3. Mathematical method for analyzing dynamic cooperativity

The dependence of fractional saturation $\theta(s)$ on the substrate concentration is always described by a ratio between polynomial numerator and polynomial denominator, whose order is either the same or less than the number of different conformations:

$$\theta(s) = \frac{\sum_{i=1}^{n} a_i s^i}{\sum_{i=0}^{n} b_i s^i}.$$

In particular, for the two-conformational models discussed in the previous sections, the polynomial order is two:

$$\theta(s) = \frac{ds + cs^2}{a + bs + cs^2}. \tag{27}$$

Rewriting Eq. (27) in terms of reciprocal fractional saturation and reciprocal substrate concentration gives Eq. (28):

$$\frac{1}{\theta(s)} = \frac{a\left(\frac{1}{s}\right)^2 + b\frac{1}{s} + c}{d\frac{1}{s} + c}. \tag{28}$$

Eq. (28) is a second order polynomial divided by a first order polynomial and therefore is called a "2/1" function of $\frac{1}{s}$.

Dividing through by the denominator gives

$$\frac{1}{\theta(s)} = \frac{bd - ac}{d^2} + \frac{a}{d}\frac{1}{s} + \frac{c(ac - (b-d)d)}{d^2\left(\frac{d}{s} + c\right)}. \tag{29}$$

The first two terms on the right hand side of Eq. (29) represent the Michaelis–Menten relation between θ and s which is approached asymptotically at low substrate concentration. The third term represents the deviation from Michaelis–Menten kinetics at high substrate concentration when $\frac{1}{s}$ is no longer large enough to make the third term negligible. The value of $ac - d(b-d)$, the numerator of the third term, is a measure of the deviation from the Michaelis–Menten relationship. When

this expression is greater than, equal to, or less than zero, apparent positive cooperativity, Michaelis–Menten behavior, or apparent negative cooperativity is observed, respectively [41].

2.4. Kinetic proofreading and specificity amplification

Noise, stochasticity, and specificity are among the most important emerging concepts in current molecular cell biology, particularly in connection with cellular processes such as gene regulation and signal transduction. Through evolution, biological organisms have acquired a repertoire of mechanisms to counteract stochasticity thus improve the accuracy of their informational processing. Kinetic proofreading theory, first developed in 1970s [23,24], has provided a concrete example of how cellular biochemical network can function as an error reduction device, suppressing noise and improving biochemical specificity between macromolecules without relying on molecular structural modification. The molecular mechanisms of the proofreading have been extensively elucidated in DNA polymerase in terms of its exonuclease activity and protein synthesis in terms of ribosome structure and kinetics. However, having the right molecular structures and biochemical reaction networks are not sufficient for the error reduction mechanism to function. The central idea of the Hopfield–Ninio theory is the necessity of a free energy source in the form of chemical potential gradient, either from GTP/GDP or from other enzymatic cofactors. Biochemical error reduction requires a continuous free energy expenditure: high grade chemical energy is transformed into low grade heat accompanied with increasing entropy [11]. The role of free energy has been conspicuously absent in the general discussions on biochemical specificity and error reduction in cell biology.

With respect to kinetic proofreading, here addresses a fundamental question: for a given amount of available free energy to a cell, in the form of ATP/ADP (or GTP/GDP) ratio, what is the thermodynamic limitation on the error reduction and specificity amplification?

2.4.1. Minimal error rate predicted by Hopfield's 1974 model

While this model was developed for the high fidelity in biosynthetic processes, the kinetic model and the idea within have a much broader cellular applications. Here we shall cast our discussion in terms of receptor–ligand association. Fig. 10 shows a schematics of a 3-state, cyclic receptor–ligand binding model. We shall denote the equilibrium association constant for the receptor–ligand complex K_a. Then the equilibrium between the empty receptor R and the activated complex RL^* is $\frac{[RL^*]^{eq}}{[R]^{eq}} = K_a[L] = \frac{k^0_{-3}[L]}{k_3} = \frac{k_{-3}}{k_3}$, where k_3 and k^0_{-3} are the dissociation and association rate constants. We shall use k_{-3} to denote the pseudo-first order rate constant $k^0_{-3}[L]$.

We now quote a few results from standard thermodynamics. The equilibrium, standard-state free energy of hydrolysis

$$\Delta G^0_{DT} = -RT \ln\left(\frac{[T]^{eq}}{[D]^{eq}}\right).$$

Furthermore, equilibrium ATP and ADP concentrations are related to rate constants:

$$\frac{[T]^{eq}}{[D]^{eq}} = \frac{k^0_{-2}[RL^*]^{eq}}{k^0_2[RL]^{eq}} = \frac{k_{-1}k^0_{-2}k_{-3}}{k_1k^0_2k_3}, \tag{30}$$

in which the second equality is due to equilibrium relation $[RL]^{eq}/[RL^*]^{eq} = k_1k_3/(k_{-1}k_{-3})$. Hence, the free energy of ATP hydrolysis in a cell,

$$\Delta G_{DT} = \Delta G^0_{DT} + RT \ln\left(\frac{[T]}{[D]}\right) = RT \ln\left(\frac{k_1k_2k_3}{k_{-1}k_{-2}k_{-3}}\right),$$

where $[T]$ and $[D]$ are cellular ATP and ADP concentrations, not at equilibrium if a cell is alive: $\Delta G_{DT} > 0$.

As the point of departure from the original work of Hopfield, we introduce a parameter, $\gamma = e^{\Delta G_{DT}/RT}$, representing the available free energy from each ATP hydrolysis:

$$\gamma = \frac{k_1k_2k_3}{k_{-1}k_{-2}k_{-3}}. \tag{31}$$

The free energy in a living cell is from the sustained physiological level of ATP (∼8 mM) and level of ADP (∼10 M). It is not from the phosphate bond of the ATP molecule: "The Pacific Ocean could be filled with an equilibrium mixture of ATP, ADP and Pi, but the ATP would have no capacity to do work" [44]. When a cardiac myocyte experiences ischemia, its ATP/ADP ratio goes down and the cellular energy is decreased.

In Fig. 10, now let us consider two possible ligands L and L' at equal concentration. We assume they are structurally related so that they have same k_1, k_2, k_{-2} and k_{-3}.

In a test tube at equilibrium (i.e., $[T] = [T]^{eq}$ and $[D] = [D]^{eq}$), then

$$\frac{k^0_1k^0_2k_3}{k_{-1}k^0_{-2}k^0_{-3}} = \frac{k'^0_1k'^0_2k'_3}{k'_{-1}k'^0_{-2}k'0_{-3}} = \frac{[D]^{eq}}{[E]^{eq}},$$

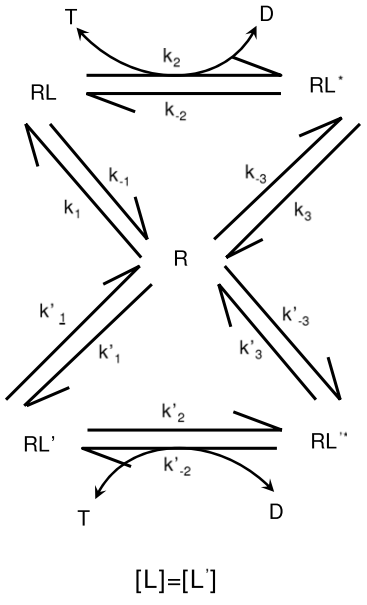

Fig. 10. A simple kinetic model of receptor–ligand binding coupled with hydrolysis reaction $T \rightleftharpoons D$. $k_{-3} = k^0_{-3}[L]$, $k_1 = k^0_1[L]$ and $k'_{-3} = k'^0_{-3}[L']$, $k'_1 = k'^0_1[L']$.

hence

$$\gamma = \frac{k_1 k_2 k_3}{k_{-1} k_{-2} k_{-3}} = \frac{k'_1 k'_2 k'_3}{k'_{-1} k'_{-2} k'_{-3}} = 1.$$

Therefore, the ratio of the two affinities at equilibrium is

$$f = \frac{\frac{[RL^*]}{[R][L]}}{\frac{[RL'^*]}{[R][L']}} = \frac{\frac{k_{-3}}{k_3}}{\frac{k_{-3}}{k'_3}} = \theta.$$

Their affinities with the receptor, however, are different due to $\frac{k'_{-1}}{k_{-1}} = \frac{k'_3}{k_3} = \theta$, where $\theta < 1$. That is L' has a higher affinity to the receptor than L; the receptor is more specific for L' than for L.

In the Hopfield's model for biosynthesis, f represents the expected error rate of a wrong amino acid being incorporated into a protein. Here, f represents the error rate of activation due to non-specific binding.

In living cells, due to the hydrolysis reaction in Fig. 10, $RL + T \rightleftharpoons RL^* + D$, $[D]$ and $[T]$ are not at their equilibrium concentrations. The error rate therefore depends on how much energy is available, i.e., f is a function of γ. Here $\gamma \neq 1$, but $\gamma = \frac{k_1 k_2 k_3}{k_{-1} k_{-2} k_{-3}} = \frac{k'_1 k'_2 k'_3}{k'_{-1} k'_{-2} k'_{-3}}$ still hold as the thermodynamic constrain.

For Hopfield 3-state, 1-cycle model,

$$f = \theta \frac{(k_1 k_2 + k_2 k_{-3} + k_{-1} k_{-3})}{(k_2 k_3 + k_3 k_{-1} + k_{-1} k_{-2})} \frac{(k_2 k_3 + \theta k_3 k_{-1} + k_{-1} k_{-2})}{(k_1 k_2 + k_2 k_{-3} + \theta k_{-1} k_{-3})}, \tag{32}$$

use relation Eq. (31) to eliminate $k_{-1}k_{-2}$ in Eq. (32), one has

$$f(\gamma) = \theta \frac{(k_1 k_2 + k_2 k_{-3} + k_{-1} k_{-3})}{\left(k_2 k_{-3} + k_{-1} k_{-3} + \frac{k_1 k_2}{\gamma}\right)} \frac{\left(k_2 k_{-3} + \theta k_{-1} k_{-3} + \frac{k_1 k_2}{\gamma}\right)}{(k_1 k_2 + k_2 k_{-3} + \theta k_{-1} k_{-3})}.$$

One useful inequality. For $\gamma > 1$, $\theta < 1$, and non-negative a's, b, and c, we have $\frac{(a+b+c)}{\left(a+\frac{b}{\gamma}+c\right)} \frac{\left(a\theta+\frac{b}{\gamma}+c\right)}{(a\theta+b+c)} \geq \left(\frac{1+\sqrt{\gamma\theta}}{\sqrt{\gamma}+\sqrt{\theta}}\right)^2$, where the equality holds true when $c = 0$ and $\frac{b}{a} = \sqrt{\gamma}\theta$.

Then we have the minimal error rate

$$f_{\min}(\gamma) = \theta \left(\frac{1 + \sqrt{\gamma\theta}}{\sqrt{\gamma} + \sqrt{\theta}}\right)^2 \tag{33}$$

for all possible rate constants with a given γ when $\frac{k_{-3}}{k_1} = 0$ and $\frac{k_1 k_2}{k_{-1}k_{-3}} = \sqrt{\gamma\theta}$. These two relations imply the inequalities

$$k_{-1} \gg k_2, \quad k_1 \gg k_{-3}, \quad \frac{k_1}{k_{-3}}\frac{k_2}{k_{-1}} > \theta, \quad k_3 > k_{-2}. \tag{34}$$

The conditions in Eq. (34) can be described, *à la* Hopfield, "wrong substrate arriving at RL^* must come typically through step 2 rather than 3" and "the rate of loss of molecules RL^* must be dominantly by path 3" [23]. $k_{-1} \gg k_2$ and $k_1 \gg k_{-3}$ imply that the step 1 is in rapid equilibrium for an optimal error reduction. When $\gamma \gg \theta^{-1}$, i.e., there is sufficient amount of energy available, $f_{\min}$ approached θ^2. This is the celebrated result of. Eq. (33) offers a more complete, quantitative description of how much error can be reduced with finite amount of energy available.

2.4.2. Absolute thermodynamic limit on error rate with finite available free energy

The $f_{\min}$ obtained above is confined within the kinetic scheme given in Fig. 10. We now seek to provide an estimation of the absolute lower bound of error rate, with a given amount of energy γ, for any possible kinetic scheme, i.e., a true thermodynamic limit irrespective of the detailed "wiring diagram".

The competition between L and L' for R can be written into a single biochemical reaction

$$L + RL'^* \rightleftharpoons L' + RL^* \tag{35}$$

which has an equilibrium constant θ. With equal amount of L and L', the free energy difference between RL^* and RL'^*, ΔG^{eq}, is zero in a chemical equilibrium:

$$\Delta G^{eq} = -RT \ln\theta + RT \ln \frac{[RL^*]^{eq}}{[RL'^*]^{eq}} = 0.$$

In living cells, this reaction is coupled to an "energy source" with free energy $RT \ln\gamma$. We have recently shown that the free energy from the source and the ΔG in Eq. (36) satisfy the Kirchhoff's loop law. Hence, the maximum contribution to the reaction, assuming there is no waste of energy in the coupling, will be

$$\Delta G = -RT \ln\theta + RT \ln \frac{[RL^*]}{[RL'^*]} = -RT \ln\gamma.$$

This yields

$$\frac{[RL^*]}{[RL'^*]} = \frac{\theta}{\gamma}. \tag{36}$$

3. Regulations and feedbacks in nonequilibrium biochemical futile cycles

Reversible phosphorylation of enzymes is perhaps one of the most important biochemical regulatory mechanisms that occur in both prokaryotic and eukaryotic organisms [45,46]. On the onset of our discussion, it is crucial to point out the term "reversible" used in the biochemical literature means the phosphorylation can be counteracted by a dephosphorylation reaction. The latter $E^* \rightarrow E + Pi$, however, is not the simple reversal of the former $E + ATP \rightarrow E^* + ADP$, where E and E^* represent the unphosphorylated and phosphorylated states of an enzyme. The two reactions are catalyzed by two different enzymes of their own: a protein kinase and a protein phosphatase, respectively. In fact, a complete phosphorylation–dephosphorylation cycle (PdPC) hydrolyzes one ATP. In a living cell, the reaction is positively driven with energy dissipation. Using a cellular phosphorylation potential of $\Delta G_{\rm ATP} = 25 k_B T$ [47], the "$\gamma (= e^{\Delta G_{\rm ATP}/k_B T})$ parameter" of a living cell is on the order of 10^{10}.

It is also important to mention that kinetically, the PdPC is isomorphic to yet another key biochemical regulatory mechanism: the GTPase reaction cycle:

$$\text{GTPase} \cdot \text{GDP} + \text{GTP} \rightarrow \text{GTPase} \cdot \text{GDP} + \text{GDP},$$
$$\text{GTPase} \cdot \text{GTP} \rightarrow \text{GTPase} \cdot \text{GDP} + \text{Pi}.$$

The two reactions are also catalyzed by two enzymes, guanine nucleotide exchange factor (GEF) and GTPase-activating proteins (GAP), respectively. If one identifies E with GTPase · GDP, E^* with GTPase · GTP, ATP and ADP with GTP and GDP, then indeed one sees the two kinetic scheme are the same. In this section, we shall use the terminology associated with the PdPC, but its applications to GTPase is obvious.

For a very long time, cyclic reactions such as PdPC and GTPase are called *futile cycles* in biochemical literature: they dissipate cellular free energy, but they do not seem to perform any function in the classical sense: mechanical work, biosynthesis, or transport against chemical gradient. These three are collectively known as the three major energy sinks in a living cell [48]. We now know that such futile cycles use free energy to process information and regulate cellular activities [35]. The nonequilibrium steady state (NESS) is the way of life [49].

This section is devoted to study biochemical regulatory processes, in particular futile cycles, from the perspective of the theory of NESS.

Reversible chemical modification of an enzyme or receptor results in a conformational change in their structures. The structural change causes them to become biochemically active (or inactive). This is quite similar to the turning on (or off) of a switch. Phosphorylation usually occurs on serine, threonine, and tyrosine residues of a protein in eukaryotic cells. One such example of the regulatory role that phosphorylation plays is on the p53 tumor suppressor protein. The p53 protein is heavily regulated and contains more than 18 different phosphorylation sites. Activation of p53 can lead to cell cycle arrest, which can be reversed under some circumstances, or apoptotic cell death. p53 activation occurs when a cell is damaged [50]. Another widely studied phosphorylation kinase cascade is mitogen-activated protein kinases (MAPK) signaling system [51].

Biological switches such as PdPC requires high switching sensitivity: the sharpness of the activation of the substrate protein (enzyme) in response to the concentration of the kinase is a key characteristics from the perspective of metabolic control analysis. The sharpness is often measured by a Hill coefficient first proposed by Hill [52]. The sharp activation in PdPC switches has always been compared to allosteric cooperative transitions [53], but it is found that the latter mechanism could hardly show positive cooperativity with Hill coefficient greater than 4, while the former multi-enzyme systems may exhibit ultrasensitivity [53–55] due to the mechanism of zeroth order kinetics of kinase and phosphatase.

What are the essential similarities and differences between these two different types of "cooperativity"? This significant question could date back to Fischer and Krebs [56,45], the 1992 Nobel Laureates who discovered protein phosphorylation as a regulatory mechanism for enzyme activity.

We have found that a new type of cooperativity termed temporal cooperativity, emerges in the signal transduction, PdPC module [57,49,58]. This kind of cooperativity in the cyclic reaction is temporal, with energy "stored" in time rather than in space as for allosteric cooperativity. It utilizes multiple kinetic cycles in time, in contrast to allosteric cooperativity that utilizes multiple subunits in a protein. Such is the origin of ultrasensitivity. In this section we shall thoroughly investigate both the deterministic (macroscopic) and stochastic (mesoscopic) models, focusing in particular on the identification of the source of cooperativity via comparing with allosterism. We assume the readers have some familiarity with the concept of equilibrium allosterism [59].

Recently, it has been shown experimentally that bistable system guaranteed by positive feedback could be converted to a monostable one exhibiting ultrasensitive graded response, and *vice versa* [60]. We shall also discuss the PdPC with a simple positive feedback which leads to bistability. Such a feedback in PdPC has been widely seen [61]: Src family kinase itself is activated by its phosphorylated substrate receptor [62]; and GEF Rabex-5 is itself activated by GTP bound Rab-5, the product of the reaction it catalyzes [63]. Both in some sense are auto-catalytic.

Even more interestingly, it has been found that the kinetic system of PdPC with feedback is equivalent to the self-regulating gene network [14]! Hence, the analysis and conclusions in this section apply to there as well. Our stochastic approach not only quantitatively characterize the relative stability of different attractors (*e.g.*, corresponding to different phenotypes), but also reveals an extremely slow stochastic time scales beyond the deterministic approach. Stochastic jumps on this time scale is highly relevant to cellular "evolution" [64], and it is implicated in cancer carcinogenesis [65].

All of these biological functions depend upon the open, driven chemical nature of the biochemical systems that are spontaneously self-organizing into the NESS. The mesoscopic approach to cellular biochemistry is not merely a refinement to the deterministic approach based on classic Law of Mass Action. It has a much more fundamental theory which reveals nontrivial emergent properties across several different time scales. In fact, the deterministic kinetics should be viewed as merely one, though a very important one at a short time scale, signature of a mesoscopic stochastic dynamics.

3.1. Reversible kinetic model for covalent modification

There is now a body of literature on theoretical analysis of the phosphorylation–dephosphorylation cycle (PdPC) catalyzed, respectively, by kinase E_1 and phosphatase E_2 [54,57,66,67,49]. Protein W is covalently modified into W^* in the phosphorylation reaction, and *vice versa*:

$$W + E_1 + \mathrm{ATP} \underset{d_1}{\overset{a_1^0}{\rightleftharpoons}} W \cdot E_1 \cdot \mathrm{ATP} \underset{q_1^0}{\overset{k_1}{\rightleftharpoons}} W^* + E_1 + \mathrm{ADP};$$

$$W^* + E_2 \underset{d_2}{\overset{a_2}{\rightleftharpoons}} W^* E_2 \underset{q_2^0}{\overset{k_2}{\rightleftharpoons}} W + E_2 + Pi.$$

With the constant concentrations of ATP, ADP and Pi inside a cell, we introduce the pseudo-first-order reaction constants $a_1 = a_1^0[\mathrm{ATP}]$, $q_1 = q_1^0[\mathrm{ADP}]$ and $q_2 = q_2^0[Pi]$, then these reactions become

$$\text{Reaction Rxn1}: \; W + E_1 \underset{d_1}{\overset{a_1}{\rightleftharpoons}} WE_1;$$

$$\text{Reaction Rxn2}: \; WE_1 \underset{q_1}{\overset{k_1}{\rightleftharpoons}} W^* + E_1;$$

$$\text{Reaction Rxn3}: \; W^* + E_2 \underset{d_2}{\overset{a_2}{\rightleftharpoons}} W^* E_2;$$

$$\text{Reaction Rxn4}: \ W^*E_2 \underset{q_2}{\overset{k_2}{\rightleftharpoons}} W + E_2.$$

From a biochemistry point of view, the intracellular phosphorylation potential through the reaction cycle, Rxn1–Rxn4 is simply an ATP hydrolysis: [57]:

$$\begin{aligned}\Delta G &= \Delta G_1 + \Delta G_2 + \Delta G_3 + \Delta G_4\\ &= k_BT \log \frac{a_1[W][E_1]}{d_1[WE_1]} + k_BT \log \frac{k_1[WE_1]}{q_1[W^*][E_1]} + k_BT \log \frac{a_2[W^*][E_2]}{d_2[W^*E_2]} + k_BT \log \frac{k_2[W^*E_2]}{q_2[W][E_2]}\\ &= k_BT \log \frac{a_1k_1a_2k_2}{d_1q_1d_2q_2} = k_BT \log \gamma,\end{aligned}$$

where $\gamma = a_1k_1a_2k_2/(d_1q_1d_2q_2)$ will be called the energy parameter. The system will be in a chemical equilibrium, if and only if $\Delta G = 0$, i.e. $\gamma = 1$. In a normal living cell, $\Delta G = 14$ kcal mol^{-1}, which corresponds to $\gamma = 10^{10}$ [47].

3.2. Complete mathematical models and nonequilibrium steady states

We start our analysis with the deterministic kinetics of a PdPC.

3.2.1. Deterministic model with the law of mass action

Biochemists usually develop a deterministic model of a biochemical system with a macroscopic view that is consistent with test tube experiments: based on the law of mass action, the forward and backward rates, i.e., fluxes, of Rxn1 are $J_1 = a_1[W][E_1]$ and $J_{-1} = d_1[WE_1]$ respectively; similarly, the forward and backward fluxes of Rxn2, Rxn3, and Rxn4 are $J_2 = k_1[WE_1], J_{-2} = q_1[W^*][E_1], J_3 = a_2[W^*][E_2], J_{-3} = d_2[W^*E_2], J_4 = k_2[W^*E_2]$ and $J_{-4} = q_2[W][E_2]$ respectively.

We can choose $[W^*]$, $[E_1]$ and $[E_2]$ as independent variables according to the three conservation laws $W_T = [W] + [WE_1] + [W^*E_2] + [W^*]$, $E_{1T} = [E_1] + [WE_1]$ and $E_{2T} = [E_2] + [W^*E_2]$, where W_T, E_{1T} and E_{2T} are constants representing the total concentrations of target protein, kinase and phosphatase respectively. Then the deterministic equations are

$$\begin{aligned}\frac{d[W^*]}{dt} &= J_2 - J_{-2} + J_{-3} - J_3;\\ \frac{d[E_1]}{dt} &= J_{-1} - J_1 + J_2 - J_{-2};\\ \frac{d[E_2]}{dt} &= J_{-3} - J_3 + J_4 - J_{-4}.\end{aligned} \tag{37}$$

In the steady state, the right-hand-side of Eq. (37) is set to be zero. This yields the important definition of the net, cycle flux $J \overset{\text{def}}{=} J_i - J_{-i},\ i = 1, 2, 3, 4$. Based on the relation

$$\gamma = \frac{a_1k_1a_2k_2}{d_1q_1d_2q_2} = \frac{J_1J_2J_3J_4}{J_{-1}J_{-2}J_{-3}J_{-4}},$$

we know that $J > 0$ is equivalent to the energy parameter $\gamma > 1$; and $J < 0$ is equivalent to $\gamma < 1$. Moreover, the entropy production rate can be expressed, in unit k_B, as

$$\text{epr} = \text{flux} \times \text{potential} = J \cdot \log \gamma.$$

Obviously, epr $= 0$ if and only if $\gamma = 1$, which means chemical equilibrium state according to the thermodynamic analysis in Section 3.2.3.

3.2.2. Stochastic model: the chemical master equation

A deterministic model, however, only describes the behavior of a system with large populations. It cannot capture the temporal fluctuations of a small biochemical system, such as a cell, with either extrinsic or intrinsic noise. Intrinsic fluctuations are determined by the structure, reaction rates, and species concentrations of the underlying biochemical networks, which always exist even when the external environment is invariant.

A stochastic chemical kinetic approach in terms of the chemical master equations (CME) will now be presented. The CME is based on reaction stoichiometry, molecular numbers, and kinetic rate constants. It describes a stochastic process with discrete states and continuous time parameter. See Part I, Section 2.3.

Denote the volume as V, which is a fixed parameter of the system. And let $N_T = W_TV$, $N_{1T} = E_{1T}V$ and $N_{2T} = E_{2T}V$, recalling $W_T = [W] + [WE_1] + [W^*E_2] + [W^*]$, $E_{1T} = [E_1] + [WE_1]$ and $E_{2T} = [E_2] + [W^*E_2]$ are constants representing the total concentrations of target protein, kinase and phosphatase respectively. So we can still choose the molecule numbers of

species W^*, E_1 and E_2 as three independent variables. Let $p(i, j, k; t)$ be the probability of the system, at time t, has molecule copy numbers i, j, and k for W^*, E_1 and E_2, respectively. Then $p(i, j, k; t)$ satisfies the *chemical master equation*

$$\begin{aligned}\frac{dp(i,j,k;t)}{dt} &= \frac{a_1}{V}(N_T - N_{1T} - N_{2T} - i + j + k + 1)(j+1)p(i, j+1, k; t)\\ &+ d_1(N_{1T} - j + 1)p(i, j-1, k; t) + k_1(N_{1T} - j + 1)p(i-1, j-1, k; t)\\ &+ \frac{q_1}{V}(i+1)(j+1)p(i+1, j+1, k; t) + \frac{a_2}{V}(i+1)(k+1)p(i+1, j, k+1; t)\\ &+ d_2(N_{2T} - k + 1)p(i-1, j, k-1; t) + k_2(N_{2T} - k + 1)p(i, j, k-1; t)\\ &+ \frac{q_2}{V}(N_T - N_{1T} - N_{2T} - i + j + k + 1)(k+1)p(i, j, k+1; t)\\ &- \Big[\frac{a_1}{V}(N_T - N_{1T} - N_{2T} - i + j + k)j + d_1(N_{1T} - j) + k_1(N_{1T} - j) + \frac{q_1}{V}ij\\ &+ \frac{a_2}{V}ik + d_2(N_{2T} - k) + k_2(N_{2T} - k) + \frac{q_2}{V}(N_T - N_{1T} - N_{2T} - i + j + k)k\Big]p(i, j, k; t).\end{aligned}$$

It is necessary to explain the transition probability rates in the above equation. When the system is in the state (i, j, k), the molecular numbers of WE_1, W^*E_2 and W are $N_{1T} - j$, $N_{2T} - k$ and $N_T - i - (N_{1T} - j) - (N_{2T} - k)$ respectively. Moreover, the parameters $(a_{1,2}/V)$ and $(q_{1,2}/V)$ are number-based, rather than concentration based, rate constants [68]. Note that $d_{1,2}$ and $k_{1,2}$ are first-order rate constants with dimension $[\text{time}]^{-1}$; while second-order rate constants $a_{1,2}$ and $q_{1,2}$ have dimension $[\text{time}]^{-1}[\text{concentration}]^{-1}$. Hence the latter involves a factor of $1/V$ in the conversion [69]. For instance, the quantity $J_1 = a_1[W][E_1]$ has the dimension of $[\text{concentration}][\text{time}]^{-1}$, hence the probability rate $J_1 \times V = a_1 V \times \frac{N_T - N_{1T} - N_{2T} - i + j + k}{V} \times \frac{j}{V} = \frac{a_1}{V}(N_T - N_{1T} - N_{2T} - i + j + k)j$ will have the dimension of molecular numbers per time, used in the CME.

The stochastic process it represents is a jump process on a three-dimensional cubic lattice of size $N_T \times N_{1T} \times N_{2T}$. The state (i, j, k) can only jump to the adjacent states $(i, j+1, k)$, $(i, j-1, k)$, $(i-1, j-1, k)$, $(i+1, j+1, k)$, $(i+1, j, k+1)$, $(i-1, j, k-1)$, $(i, j, k-1)$ and $(i, j, k+1)$.

In probability theory, such a random-walk model is called the three-dimensional birth-and-death process, which is a special Markov chain. Generally speaking, ξ and η represent the states and $q_{\xi\eta}$ is the transition density along the passage $\xi \to \eta$. The Eq. (38) is just the Kolmogorov forward equation of the continuous-time Markov chain with transition density matrix $Q = (q_{\xi\eta})$

$$\frac{dp(\xi, t)}{dt} = p(\xi, t)Q, \tag{38}$$

where $\xi = (\xi^1, \xi^2, \xi^3)$ represents the state in which the molecule numbers of W^*, E_1 and E_2 are ξ^1, ξ^2 and ξ^3 respectively, and

$$q_{\xi\eta} = \begin{cases} \frac{a_1}{V}(N_T - N_{1T} - N_{2T} - i + j + k)j & \xi = (i, j, k), \eta = (i, j+1, k),\\ d_1(N_{1T} - j) & \xi = (i, j, k), \eta = (i, j-1, k),\\ k_1(N_{1T} - j) & \xi = (i, j, k), \eta = (i-1, j-1, k),\\ \frac{q_1}{V}ij & \xi = (i, j, k), \eta = (i+1, j+1, k),\\ \frac{a_2}{V}ik & \xi = (i, j, k), \eta = (i+1, j, k+1),\\ d_2(N_{2T} - k) & \xi = (i, j, k), \eta = (i-1, j, k-1),\\ k_2(N_{2T} - k) & \xi = (i, j, k), \eta = (i, j, k-1),\\ \frac{q_2}{V}(N_T - N_{1T} - N_{2T} - i + j + k)k & \xi = (i, j, k), \eta = (i, j, k+1),\\ -\sum_{\zeta \neq \xi} q_{\xi\zeta} & \xi = \eta = (i, j, k),\\ 0 & \text{else.}\end{cases}$$

The theory developed in Part I, Section 2.3 for Q-processes can be directly applied to the CME.

3.2.3. Nonequilibrium steady state

In Section 2 of Part I, we have discussed the Kolmogorov cycle condition for a Q-process. It was shown that it is equivalent to the time reversibility of a Markov chain, corresponding to the equilibrium steady state. The significance of this condition is that it allows one to directly write down the condition for reversibility without first deriving the steady state. Although

there are many cycles in the Markov chain model (38), every large cycle can be decomposed into several basic four-state cycles

$$\xi_1 = (i, j, k) \to \xi_2 = (i, j-1, k) \to \xi_3 = (i+1, j, k) \to \xi_4 = (i, j, k-1) \to \xi_1 = (i, j, k),$$

which corresponds precisely to the phosphorylation–dephosphorylation chemical kinetic cycle Rxn1–Rxn4.[3]

In this case, the necessary and sufficient condition for the steady state being in equilibrium, i.e. the Kolmogorov cycle condition, is expressed as $q_{\xi_1\xi_2}q_{\xi_2\xi_3}q_{\xi_3\xi_4}q_{\xi_4\xi_1} = q_{\xi_1\xi_4}q_{\xi_4\xi_3}q_{\xi_3\xi_2}q_{\xi_2\xi_1}$. From Eq. (38), this is just

$$\begin{aligned}&\frac{a_1}{V}(N_T - N_{1T} - N_{2T} - i + j + k)j \times k_1(N_{1T} - j + 1) \times \frac{a_2}{V}(i+1)kk_2(N_{2T} - k + 1)\\ &\quad = \frac{q_2}{V}(N_T - N_{1T} - N_{2T} - i + j + k)kd_2(N_{2T} - k + 1) \times \frac{q_1}{V}(i+1)j \times d_1(N_{1T} - j + 1).\end{aligned}$$

One can derive from this $\gamma \triangleq a_1k_1a_2k_2/(d_1q_1d_2q_2) = 1$.

Namely, $\gamma \neq 1$ is equivalent to the fact that this system is in a nonequilibrium steady state.

3.3. Reduced mathematical models

In many biochemically realistic situations, it is safe to suppose that the total concentration of W and W^* together, W_T, is much larger than that of the kinase and the phosphatase, i.e. $W_T = [W] + [W^*] \gg E_{1T}, E_{2T}$ [54,57]. Therefore, we can reasonably assume that the time scale for the enzymes E_1 and E_2 to reach steady state is much faster than the dynamics of W and W^*. Consequently, the concentrations of W and W^* can be treated as constant when studying the dynamics of kinase E_1 and phosphatase E_2. And when studying the dynamics of W and W^*, E_1 and E_2 can be treated as in their steady states. This argument, known as Michaelis–Menten quasi-steady-state approximation, can be rigorously justified using the method of singular perturbation [66]. The single-molecule approach presented in the previous section, of course, is the ultimate case of "low enzyme concentration with high substrate concentration". It yields Michaelis–Menten's result exactly.

Therefore, the dynamics of kinase and phosphatase can be considered separably:

$$\begin{aligned}&\text{(a)}: W + E_1 \underset{d_1}{\overset{a_1}{\rightleftharpoons}} WE_1 \underset{q_1}{\overset{k_1}{\rightleftharpoons}} W^* + E_1,\\ &\text{(b)}: W + E_2 \underset{k_2}{\overset{q_2}{\rightleftharpoons}} W^*E_2 \underset{a_2}{\overset{d_2}{\rightleftharpoons}} W^* + E_2.\end{aligned} \tag{39}$$

The steady states in the above Michaelis–Menten kinetics is well-known in the classic enzyme kinetics [37]. The fluxes from W to W^* and from W^* to W in reactions (a) and (b) of Eq. (39) are respectively

$$v_1([W]) = \frac{\frac{V_1[W]}{K_1}}{1 + \frac{[W]}{K_1} + \frac{[W^*]}{K_1^*}}, \qquad v_1^*([W^*]) = \frac{\frac{V_1^*[W^*]}{K_1^*}}{1 + \frac{[W]}{K_1} + \frac{[W^*]}{K_1^*}}, \tag{40}$$

and

$$v_2([W]) = \frac{\frac{V_2[W]}{K_2}}{1 + \frac{[W]}{K_2} + \frac{[W^*]}{K_2^*}}, \qquad v_2^*([W^*]) = \frac{\frac{V_2^*[W^*]}{K_2^*}}{1 + \frac{[W]}{K_2} + \frac{[W^*]}{K_2^*}}, \tag{41}$$

under time-scale separation, in which the parameters $V_1 = k_1E_{1T}$, $V_1^* = d_1E_{1T}$, $V_2 = d_2E_{2T}$ and $V_2^* = k_2E_{2T}$ are the maximal forward ($W \to W^*$) and backward ($W^* \to W$) fluxes of the reactions (a) and (b); and $K_1 = \frac{d_1+k_1}{a_1}$, $K_2^* = \frac{d_2+k_2}{a_2}$, $K_1^* = \frac{d_1+k_1}{q_1}$, $K_2 = \frac{d_2+k_2}{q_2}$ are the corresponding Michaelis constants. The energy parameter, then,

$$\gamma = \frac{a_1k_1a_2k_2}{d_1q_1d_2q_2} = \frac{V_1K_1^*V_2^*K_2}{V_1^*K_1V_2K_2^*} \equiv \frac{v_1([W])v_2^*([W^*])}{v_2([W])v_1^*([W^*])}, \tag{42}$$

which is independent of $[W]$ and $[W^*]$.

With the Michaelis–Menten (MM) approximation, Eqs. (40)–(42) now give a reduced kinetic model for the original PdPC, as shown in Fig. 11(A) [58,66]. The reaction scheme can be modeled as deterministic kinetics [57], or stochastic kinetics as shown on the right side of Fig. 11(A). See [11] why one can still consider exponential waiting time in the Markov chain with the MM rates.

$$W \underset{f_2([W^*])}{\overset{f_1([W])}{\rightleftharpoons}} W^*, \tag{43}$$

where $f_1([W]) = v_1([W]) + v_2([W])$ is the instantaneous total flux from W to W^*, and $f_2([W^*]) = v_1^*([W^*]) + v_2^*([W^*])$ is the total, instantaneous flux from W^* to W, and $[W] + [W^*] = W_T$, a constant.

[3] Other ordering of these reactions could also form other cycles. But they all lead to the same result.

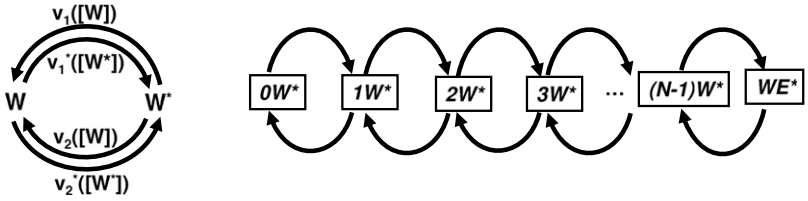

(A) Temporal cooperativity: W(unphosphorylated protein), W^*(phosphorylated protein).

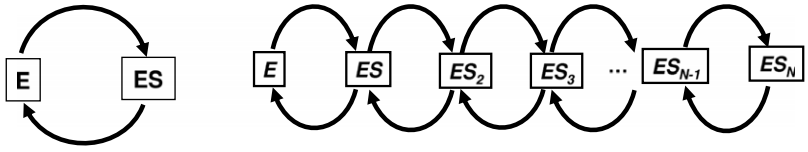

(B) Allosteric cooperativity: E(unoccupied state of sites), ES(occupied state of sites).

Fig. 11. (A) The reduced model of PdPC switch and the illustration of its corresponding chemical master equation; (B) The general model of allosteric cooperativity and the illustration of its corresponding chemical master equation.

3.3.1. Deterministic model

The ordinary differential equation of the model (43) is

$$\frac{d[W^*]}{dt} = f_1(W_T - [W^*]) - f_2([W^*]), \tag{44}$$

whose steady state $[W^*]^{ss}$ satisfies $f_1(W_T - [W^*]^{ss}) = f_2([W^*]^{ss})$ and $[W]^{ss} = W_T - [W^*]^{ss}$.

What we concern most is the steady state fraction of phosphorylated protein W^*, i.e. $\phi = [W^*]^{ss}/W_T$.

Beard and Qian [66] have written down the general equation for ϕ in the deterministic model under the assumption $W_T \gg E_{1T} + E_{2T}$:

$$\theta = \frac{\mu\gamma[\mu - (\mu+1)\phi]\left(\phi - \frac{K_1^*(W_T+K_1)}{(K_1^*-K_1)W_T}\right)K_2K_2^*(K_1^* - K_1)}{[\mu\gamma - (\mu\gamma+1)\phi]\left(\phi + \frac{K_2^*(W_T+K_2)}{(K_2-K_2^*)W_T}\right)K_1K_1^*(K_2 - K_2^*)},$$

where

$$\theta = \frac{V_1K_2^*}{K_1V_2^*}, \qquad \mu = \frac{V_2K_2^*}{K_2V_2^*}, \qquad \gamma = \frac{V_1K_1^*V_2^*K_2}{V_1^*K_1V_2K_2^*} = \frac{a_1k_1a_2k_2}{d_1q_1d_2q_2}.$$

In most biochemical applications, we have $K_1^* \gg K_1, K_2 \gg K_2^*K_2 \gg W_T$ (i.e. $q_1, q_2 \ll 1$), then $K_1^* - K_1 \approx K_1^*, K_2 - K_2^* \approx K_2, W_T + K_2 \approx K_2$, so the above equation can be simplified to [57]

$$\sigma \overset{\text{def}}{=} \frac{\theta K_1}{K_2^*} = \frac{V_1}{V_2^*} = \frac{\mu\gamma[\mu - (\mu+1)\phi]\left(\phi - 1 - \frac{K_1}{W_T}\right)}{[\mu\gamma - (\mu\gamma+1)\phi]\left(\phi + \frac{K_2^*}{W_T}\right)}. \tag{45}$$

If we let the free energy parameter γ tends to infinity, then $\mu = 0$ (i.e. $q_1 = q_2 = 0$). From Eq. (45), one can get

$$\sigma = \frac{\phi\left(1 - \phi + \frac{K_1}{W_T}\right)}{(1-\phi)\left(\phi + \frac{K_2^*}{W_T}\right)},$$

which is just the celebrated Goldbeter–Koshland equation [54] in their pioneer work on zero-order ultrasensitivity.

However, in such a deterministic model, the concentrations of phosphorylated protein W and its dephosphorylated state W^* are both the ensemble-averaged quantities. It is unable to adequately reveal the intrinsic essence of temporal cooperativity.

3.3.2. Stochastic model: chemical master equation

In order to illustrate the essence of "cooperativity" – usually biochemists think certain kind of cooperative behavior is responsible for a sharp transition – we now turn to the stochastic model based on the chemical master equation. Let V be the volume of the system, then the total molecule number of W and W^* is $N = W_TV$. Due to the existence of stochastic fluctuations, one can no longer determine the molecule numbers of a species at a given time t, and rather only determine

the probability of the copy numbers of W^* being i (the copy number of W then will be $N-i$). According to the mechanism (43), the chemical master equation model is illustrated on the right side of Fig. 11(A).

Denote the probability of the state iW^* at time t as $p(i,t)$, then it satisfies the following equation

$$\begin{aligned}
\frac{dp(0,t)}{dt} &= f_2(1/V)Vp(1;t) - f_1(N/V)Vp(0,t);\\
\frac{dp(i,t)}{dt} &= f_1((N+1-i)/V)Vp(i-1,t) + f_2((i+1)/V)Vp(i+1,t)\\
&\quad - [f_1((N-i)/V) + f_2(i/V)]Vp(i,t), \quad i = 1,2,\ldots,N-1;\\
\frac{dp(N,t)}{dt} &= f_1(1/V)Vp(N-1,t) - f_2(N/V)Vp(N,t).
\end{aligned} \tag{46}$$

It needs to be emphasized that from a purely mathematical standpoint, the stochastic model in Eq. (46) satisfies the detailed balance condition. However, the detailed balance condition of this reduced model does not imply the underlying, original chemical system has detailed balance. The reversibility (i.e., equilibrium) of the complete model (i.e. $\gamma = 1$) is not equivalent to the reversibility of the reduced model. Rather, $\gamma = 1$ corresponds to non-cooperativity, as we shall show below.

The stationary probability of the state iW^* in Fig. 11(A) is

$$P^{ss}(i) = \frac{\prod_{j=1}^{i} \frac{f_1((N+1-j)/V)}{f_2(j/V)}}{1 + \sum_{i=1}^{N}\prod_{j=1}^{i} \frac{f_1((N+1-j)/V)}{f_2(j/V)}}, \tag{47}$$

and the averaged molecule number of W^* is

$$\langle W^*\rangle = \frac{\sum_{i=1}^{N} i\prod_{j=1}^{i} \frac{f_1((N+1-j)/V)}{f_2(j/V)}}{1 + \sum_{i=1}^{N}\prod_{j=1}^{i} \frac{f_1((N+1-j)/V)}{f_2(j/V)}}. \tag{48}$$

Similar to the deterministic model, we introduce the ratio of the averaged molecule number $\langle W^*\rangle$ of phosphorylated protein molecules and the total molecule number N,

$$\langle\phi\rangle \overset{\text{def}}{=} \frac{\langle W^*\rangle}{N} = \frac{\sum_{i=1}^{N} i\prod_{j=1}^{i} \frac{f_1((N+1-j)/V)}{f_2(j/V)}}{N\left(1 + \sum_{i=1}^{N}\prod_{j=1}^{i} \frac{f_1((N+1-j)/V)}{f_2(j/V)}\right)}. \tag{49}$$

In the following sections, one could see that compared with the deterministic ϕ, the stochastic averaged $\langle\phi\rangle$ not only keeps the thermodynamic properties, but also reveals the temporal variance of the molecule numbers and is easy to be compared with the allosteric cooperativity.

3.3.3. Analogous equilibrium constants

In order to estimate the degree of cooperative phenomenon in the PdPC switch, we introduce the "equilibrium constants" similar to the Adair constants [37] in the allosteric cooperative phenomenon.

For the state $(j-1)W^*$, there have already been $(j-1)$ molecules transited from W to W^*, thus there are $(N+1-j)$ ways of transiting for the next molecule of W to W^*. Similarly, for the state jW^*, there have already been j molecules transited from W to W^*, and there are j ways of transiting for the next molecule of W^* back to W.

Introducing quantities $K_j = [(N+1-j)f_2(j/V)]/[jf_1((N+1-j)/V)]$, representing the "de-activation capability" of the j-th molecule in the state $(N-j,j)$ transiting back from the activated state W^* to the inactive state W, which will be called "de-activation constants". Their reciprocals will be called "activation constants", representing the j-th molecule transiting from the inactive state W to the activated state W^*.

So here one could rewrite the formula (49) by the de-activation constants as

$$\langle\phi\rangle = \frac{\sum_{i=1}^{N} \frac{(N-1)!}{(i-1)!(N-i)!}\frac{1}{\prod_{j=1}^{i} K_j}}{1 + \sum_{i=1}^{N} \frac{N!}{i!(N-i)!}\frac{1}{\prod_{j=1}^{i} K_j}},$$

which is essentially same as the general Adair scheme (50) of allosteric cooperativity.

Comparing with the classical allosteric cooperativity (Fig. 11(B)), we know there exists the temporal cooperative phenomenon if the quantities $\{K_j,\ j = 1, 2, \ldots, N\}$ successively decreases, implying the more number of molecules of W^* is, the larger the activation constant of the next molecule transiting from the state W to W^* becomes. Furthermore, the cooperative phenomenon appears more and more distinct when the gradient of the decreasing quantities $\{K_j,\ j = 1, 2, \ldots, N\}$ increases.

3.4. Switching behavior

3.4.1. Non-driven chemical system ($\gamma = 1$): no switch

While sensitivity amplification requiring both nonlinearity and nonequilibrium is intuitively obvious [70,71], the above analysis offers a more quantitative understanding of such systems [57,49], which partially answered the question posed by Fischer and Krebs. One essential difference between the allosteric mechanism and the hydrolysis cycle, it suggests, is that the former does not expend energy but requires large mass: "The costs of the two types of regulations are quite different. One requires a significant amount of regulator biosynthesis in advance. The other requires only a small amount of regulators for the hydrolysis reaction, but it consumes energy during the regulation" [49].

One could build both of the deterministic and stochastic models for this biochemical system, which share two different perspectives: the deterministic looks for sharpness and stochastic looks for large fluctuations. Furthermore, both of them reveal the same thermodynamic property, and are complementary to each other.

3.4.1a. The deterministic model. When $\gamma = 1$, this system is in chemical equilibrium state and we have

$$\frac{f_1([W])}{f_2([W^*])} = \frac{v_1([W])}{v_1^*([W^*])} = \frac{v_2([W])}{v_2^*([W^*])} = \mu\frac{[W]}{[W^*]},$$

recalling $\mu = d_2q_2/a_2k_2$ is a constant. Hence, we get $\phi = \mu/(\mu + 1)$ is a constant, which does not vary with the concentrations of the kinase and phosphatase. It implies the PdPC switch is a nonequilibrium phenomenon ($\gamma \neq 1$), which confirms the significant assertion that biological signal amplification needs energy.

3.4.1b. The stochastic model. The same conclusion also holds in the stochastic model. If $\gamma = 1$, then

$$\frac{f_1([W])}{f_2([W^*])} = \frac{v_1([W])}{v_1^*([W^*])} = \frac{v_2([W])}{v_2^*([W^*])} = \mu\frac{[W]}{[W^*]},$$

and the steady distribution of the state iW^* is $\binom{N}{i}\mu^i/(1+\mu)^N$ (Binomial distribution), so

$$\langle\phi\rangle = \frac{\langle W^*\rangle}{N} = \frac{\sum_{i=1}^{N} i\frac{N!}{i!(N-i)!}\mu^i}{N\left(1 + \sum_{i=1}^{N}\frac{N!}{i!(N-i)!}\mu^i\right)} = \frac{\mu}{1+\mu},$$

which is the same as the quantity ϕ in the deterministic model and also implies that the amplification of sensitivity is completely abolished.

Further, the de-activation constants $\{K_i,\ 1 \le i \le N\}$ are all equal to $\frac{1}{\mu}$, completely independent upon the concentrations of kinase and phosphatase: there is no cooperativity.

3.4.2. Simple PdPC switch with first-order approximation

Suppose $W_T \ll K_1, K_2^* \ll K_1^*, K_2$ (non-saturated), then

$$f_1([W]) = v_1([W]) + v_2([W]) \approx \frac{V_1[W]}{K_1} + \frac{V_2[W]}{K_2},$$

and

$$f_2([W^*]) = v_1^*([W^*]) + v_2^*([W^*]) \approx \frac{V_2^*[W^*]}{K_2^*} + \frac{V_1^*[W^*]}{K_1^*},$$

are both first-order, which is just the ordinary PdPC switch discussed in [49].

The steady state of the deterministic model is $[W]^{ss} = \frac{W_T}{1+\alpha}$ and $[W^*]^{ss} = \frac{W_T\alpha}{1+\alpha}$, where $\alpha = \frac{\frac{V_1}{K_1}+\frac{V_2}{K_2}}{\frac{V_2^*}{K_2^*}+\frac{V_1^*}{K_1^*}}$. Also since $\phi - 1 - \frac{K_1}{W_T} \approx -\frac{K_1}{W_T}$ and $\phi + \frac{K_2^*}{W_T} \approx \frac{K_2^*}{W_T}$, Eq. (45) is reduced to

$$\theta = \frac{V_1K_2^*}{V_2^*K_1} = \frac{\mu\gamma[(\mu+1)\phi - \mu]}{[\mu\gamma - (\mu\gamma+1)\phi]}$$

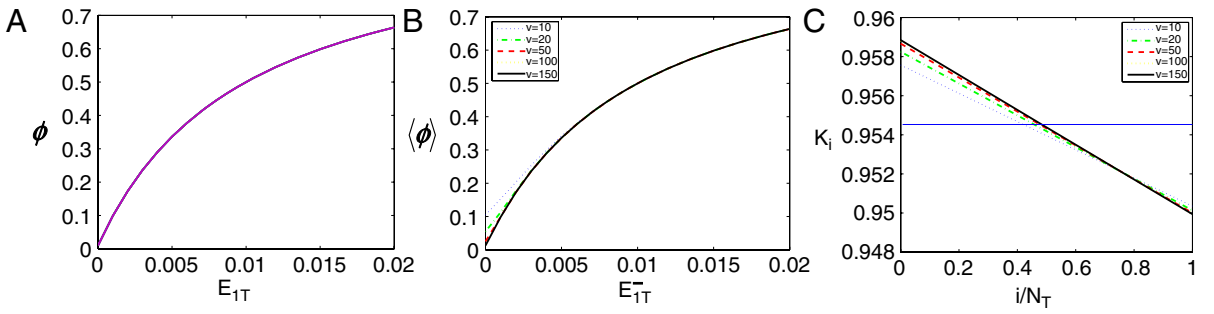

Fig. 12. (A)The curve of ϕ with respect to E_{1T} in the deterministic model of the simple PdPC switch without the first-order linear approximation; (B) The curve of $\langle\phi\rangle$ with respect to E_{1T} in the stochastic model of the simple PdPC switch without the first-order linear approximation at different volumes; (C) The dissociation constants in the simple PdPC switch with different volumes, where $a_1 = 0.01$; $d_1 = 1$; $k_1 = 1$; $q_1 = 0.0001$; $E_{1T} = 0.01$; $a_2 = 0.01$; $d_2 = 1$; $k_2 = 1$; $q_2 = 0.0001$; $E_{2T} = 0.01$; $W_T = 1$, and $\alpha = (V_1/K_1 + V_2/K_2)/(V_1/K_1 + V_2/K_2) = 1$. The horizontal line represents the quantity $1/\alpha$, which equals all the dissociation constants under the first-order assumption.

i.e.

$$\phi = \frac{\theta + \mu}{\theta + \mu + \theta/(\mu\gamma) + 1} = \frac{\alpha}{1+\alpha}.$$

In the stochastic model, the steady distribution of the state iW^* is (from Eq. (47)) $\frac{N!}{i!(N-i)!}\alpha^i/(1+\alpha)^N$ (Binomial distribution), then

$$\langle\phi\rangle = \frac{\langle W^*\rangle}{N} = \frac{\sum_{i=1}^{N} i\frac{N!}{i!(N-i)!}\alpha^i}{N\left(1+\sum_{i=1}^{N}\frac{N!}{i!(N-i)!}\alpha^i\right)} = \frac{\alpha}{1+\alpha},$$

which is the same as the quantity ϕ in the deterministic model.

Furthermore, $\alpha = \frac{\frac{V_1}{K_1}+\frac{V_2}{K_2}}{\frac{V_2^*}{K_2^*}+\frac{V_1^*}{K_1^*}}$ is an increasing hyperbolic function of E_{1T}. So $\langle\phi\rangle = \phi$ is also an increasing hyperbolic function of E_{1T} illustrating no cooperative effect either, which implies that the N molecules of W and W^* are all independent.

The variance of the molecule number of W^* is $\Sigma = \frac{\alpha}{(1+\alpha)^2}W_T V$, so the relative standard error is $\frac{\sqrt{\Sigma}}{\phi V} = \sqrt{\frac{W_T}{\alpha V}} \to 0$ when $V \to \infty$, according to the mathematical theory of Kurtz [69].

Fig. 12(A) illustrates the curve of ϕ with respect to E_{1T} based on the formula (49) of the deterministic model (44) of the simple PdPC switch without the first-order linear approximation. It presents a simple hyperbolic curve, implying non-cooperative effect. Fig. 12(B) illustrates the curves of $\langle\phi\rangle$ with respect to E_{1T} in the stochastic model (46) of the simple PdPC switch without the first-order linear approximation at different volumes, all of which also presents the simple hyperbolic shape. Fig. 12(C) represents the dissociation constants $\{K_i\}$ of temporal cooperativity with different volumes. It is found that in such a simple PdPC switch, these dissociation constants are all very close to 1 regardless of the variety of volumes, reconfirming no obvious cooperative phenomenon.

3.4.3. *Ultrasensitive PdPC switch with zeroth-order approximation*

Suppose $K_2, K_1^* \gg W_T \gg K_1, K_2^*$ (saturated), and $K_2^* \ll K_2, K_1 \ll K_1^*$, one can arrive at the limit case $\left(\frac{[W^*]}{K_1^*} \approx 0 \text{ and } \frac{[W]}{K_2} \approx 0\right)$

$$f_1([W]) = v_1([W]) + v_2([W]) \approx V_1,$$

and

$$f_2([W^*]) = v_1^*([W^*]) + v_2^*([W^*]) \approx V_2^*.$$

These are both in zeroth-order case. This is just the situations of ultrasensitive PdPC switch discussed in [57] and zero-order ultrasensitivity phenomenon put forward by Goldbeter and Koshland [54]. The Hill coefficient of the response curve can approach thousands and tens of thousands. It is worth pointing out that such a limit case can only be achieved when $\gamma \neq 1$, since otherwise $V_1^* V_2 \gg V_1 V_2^*$ which contradicts the zero-order approximation.

In the deterministic model of this limit case, we have $\phi = \delta_{\{V_1 > V_2^*\}}$, which is a step function with ideal infinite sensitivity. And in the stochastic model, the steady distribution of the state $(N-i, i)$ is $\frac{\alpha^i}{N\left(1+\sum_{i=1}^{N}\alpha^i\right)}$ (truncated geometric distribution),

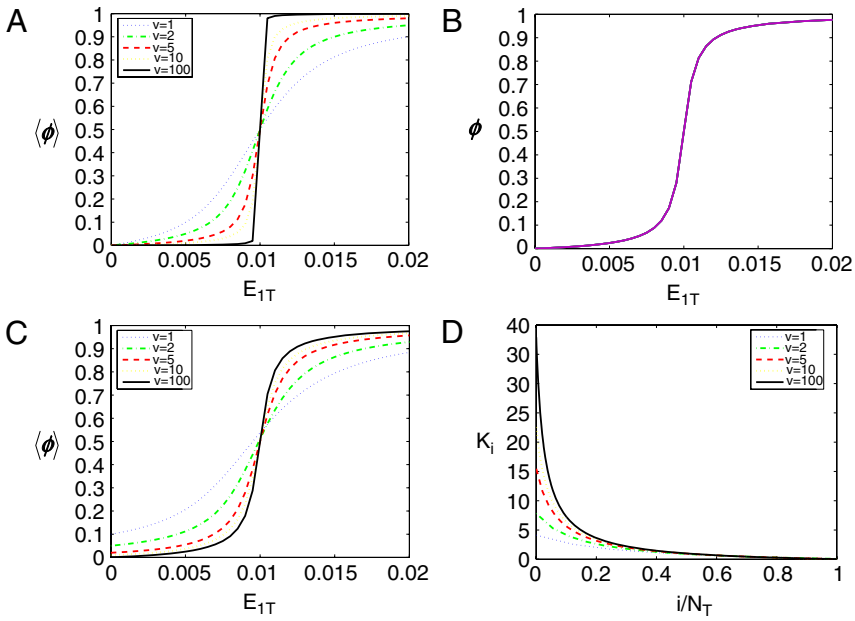

Fig. 13. (A) The curve of $\langle\phi\rangle$ with respect to E_{1T} at different volumes in the stochastic model of ultrasensitive PdPC switch under the zero-order approximation; (B) The curve of ϕ with respect to E_{1T} in the deterministic model of the ultrasensitive PdPC switch without the zero-order approximation; (C) The curve of $\langle\phi\rangle$ with respect to E_{1T} of different volumes in the stochastic model of the ultrasensitive PdPC switch without the zero-order approximation; (D) The dissociation constants in the ultrasensitive PdPC switch, where $a_1 = 10$; $d_1 = 1$; $k_1 = 1.5$; $q_1 = 0.0001$; $E_{1T} = 0.01$; $a_2 = 10$; $d_2 = 1$; $k_2 = 1.5$; $q_2 = 0.0001$; $E_{2T} = 0.01$; $W_T = 10$; and $\alpha = V_1/V_2^*$.

so

$$\langle\phi\rangle = \frac{\langle W^*\rangle}{N} = \frac{\sum_{i=1}^{N} i\alpha^i}{N\left(1+\sum_{i=1}^{N}\alpha^i\right)} = \begin{cases} \dfrac{N\alpha^{N+1} - \frac{\alpha^{N+1}-\alpha}{\alpha-1}}{N(\alpha^{N+1}-1)} & \alpha \neq 1; \\ 1/2 & \alpha = 1, \end{cases}$$

where $\alpha = \frac{V_1}{V_2^*}$ is the ratio of the forward flux from W to W^* and the backward flux from W^* to W.

Obviously, $\langle\phi\rangle$ is an increasing function of α, and consequently an increasing function of E_{1T}. And when $N \to \infty$, one has $\langle\phi\rangle \to 1$, if $\alpha > 1$; $\langle\phi\rangle \to 0$, if $\alpha < 1$. The classical Hill coefficient in this case $n_H = 2\frac{d\log\langle\phi\rangle}{d\log\alpha}\Big|_{\langle\phi\rangle=\frac{1}{2}} = \frac{1}{3}N + \frac{2}{3}$. Therefore, when the total molecule number N tends to infinity, the Hill coefficient can increase to an arbitrary value.

Hence, when the Michaelis constants K_1, K_2 are quite small, the ultrasensitive cooperative phenomenon emerges both in deterministic and stochastic perspectives, although their sensitivities cannot be as high as in the limit case discussed above.

Firstly, we investigate the cooperative phenomenon in the limit case of zero-order approximation.

Fig. 13(A) illustrates the curves of $\langle\phi\rangle$ with respect to E_{1T} at different volumes in the stochastic model of ultrasensitive PdPC switch under the zero-order approximation, in which it is found that the sensitivities of these curves are increasing with the volumes (molecule numbers) and finally approaches the ideal jumping curve of ϕ with infinite sensitivity.

Secondly, we turn to discuss the cooperative phenomenon without the zero-order approximation.

Fig. 13(B) illustrates the curve of ϕ with respect to E_{1T} based on Eq. (49) in the deterministic model (44) of the ultrasensitive PdPC switch without the zero-order approximation, whose sensitivity is less than that in Fig. 13(A) but much larger than that in Fig. 12(A). Fig. 13(C) illustrates the curves of $\langle\phi\rangle$ with respect to E_{1T} at different volumes in the stochastic model (46) by formula (49) of the ultrasensitive PdPC switch without the zero-order approximation, in which it is found that the sensitivities of these curves are increasing with the volumes (molecule numbers). Fig. 13(D) represents the dissociation constants $\{K_i\}$ of cooperativity with different volumes. It is found that in the ultrasensitive PdPC switch, these dissociation constants clearly decrease, and the gradient increases with the total molecule numbers, suggesting more and more distinct cooperative phenomenon.

3.5. Mathematical equivalence to allosteric cooperativity

Let us now turn to show an equivalence between the underlying mathematics in temporal cooperativity and in allosteric cooperativity, both of which can be expressed by "dissociation constants", which also articulates the essential differences between the simple and ultrasensitive PdPC switches (Figs. 12 and 13).

Fig. 11(B) is the general model of allosteric cooperative phenomenon including both the famous MWC and KNF models [72–74], which can all be expressed by the Adair scheme, first proposed by Adair [75] in relation to the binding of oxygen to hemoglobin. In this model, the concentration of the substrate S is fixed, and the state ES_i represents the state in which there are i sites occupied with substrates among the total N sites.

It is very important to point out that Fig. 11(A) and (B) are just the same, while the temporal cooperativity is on the scale of the N sequential phosphorylation–dephosphorylation cycles. The sequential states in Fig. 11(A) are adjacent in time rather than in space which is the case in allosteric cooperativity.

Although there is no direct interaction between the substrate enzymes, the total N molecules of W and W^* are not really independent: they all compete for the single kinase and phosphatase and hence there are implicit interactions between them. Because this interaction is not through space, but instead is sequential in time, so in [57,11] one of us referred it as temporal cooperativity.

Moreover, the meanings of the quantity N in Fig. 11(A) and (B) are totally different: the former represents the total molecule number in the temporal cooperativity model and the latter represents the total number of sites on a single enzyme molecule respectively. Hence, the degree of allosteric cooperativity is restricted by the total number of sites in a single enzyme molecule which cannot be very high (see Eq. (50)) and freely regulated, while temporal cooperativity is only restricted by the total molecule number of the target protein which can be regulated in a wide range and gives rise to the ultrasensitivity phenomenon.

Cooperativity can be generally considered in relation to the Adair scheme, and the general form of Adair equation is

$$\phi = \frac{\sum_{i=1}^{N} \frac{(N-1)!}{(i-1)!(N-i)!} \frac{c^i}{\prod_{j=1}^{i} K_j}}{1 + \sum_{i=1}^{N} \frac{N!}{i!(N-i)!} \frac{c^i}{\prod_{j=1}^{i} K_j}},$$

where $c = [S]$, $K_j = \frac{(N-j+1)c[ES_{j-1}]}{j[ES_j]}$ is the dissociation constant of the jth molecule of the substrate (regardless of site).

Consequently, there is an important corollary, that is the Hill coefficient of the $[S] - \phi$ curve determined by the Adair equation cannot exceed the total number N of sites on a single enzyme, i.e.

$$\begin{aligned} n_H &= 2\frac{d\log\phi}{d\log c}\bigg|_{\phi=\frac{1}{2}} \\ &= \left[\frac{4\sum_{i=1}^{N} i \frac{(N-1)!}{(i-1)!(N-i)!} \frac{c^i}{\prod_{j=1}^{i} K_j}}{1 + \sum_{i=1}^{N} \frac{N!}{i!(N-i)!} \frac{c^i}{\prod_{j=1}^{i} K_j}} - 4N(\phi)^2 \right]\bigg|_{\phi=\frac{1}{2}} \\ &\le [4N\phi - 4N(\phi)^2]|_{\phi=\frac{1}{2}} = N. \end{aligned} \tag{50}$$

Hence, the degree of allosteric cooperativity is restricted by the total number of sites in a single enzyme molecule which cannot be freely regulated, while temporal cooperativity is only restricted by the total molecule number of the target protein which can be regulated in a wide range and gives rise to the ultrasensitivity phenomenon. That is just why the organisms find it advantageous to develop the mechanism of covalent modification via phosphorylation and *ATP* hydrolysis to control the biological activity of proteins rather than the mechanism of allosteric transitions. Possibly, it partly answers the question of Fischer and Krebs.

Therefore, the improving of the total number of molecules of target protein cannot increase the degree of allosteric cooperativity, while it can obviously increase the degree of temporal cooperativity, indicated by the increasing gradients of the fractional saturation function $\langle\phi\rangle$ (Fig. 13(C)) and the decreasing dissociation constants $\{K_j,\ j = 1, 2, \ldots, N\}$ (Fig. 13(D))!

3.6. PdPC with positive feedback

So far, we have discussed the phenomenon of ultrasensitivity in the reversible PdPC. There, the greatest cooperativity possible in a response curve, i.e., $\langle\phi\rangle$ as a function of E_{1T} as in Fig. 13, will be a step-function. Bistable systems, however, can have a response curve not even monotonic. We now turn to discuss bistability caused by additional positive feedback in a PdPC network. And further from Fig. 14, one could easily see that the PdPC with feedback is equivalent to the self-regulating gene problem [12,14,15], which could always exhibits bistability too. In particular, we shall consider the case of positive feedback with a dimer ($\chi = 2$) (see Fig. 15(A) and (B) for detailed kinetic scheme). All the analysis below can be transported to the case of gene expression system with $\chi = 2$ in Fig. 14(A). On the other hand, it has been shown that for $\chi = 0$, 1, the

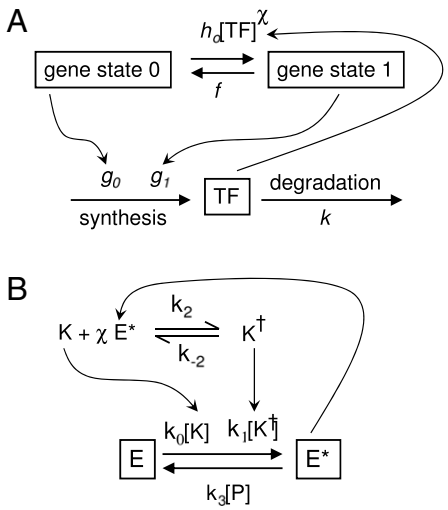

Fig. 14. Two almost isomorphic biochemical networks involved in gene regulation and cellular signaling. (A) A transcription factor (TF) is the gene product which regulates its own gene expression as a monomer or dimer ($\chi = 1, 2$). $g_0 > g_1$ and $g_0 < g_1$ correspond to a repressor and an activator, respectively. (B) A protein phosphorylation system catalyzed by a kinase K and a phosphatase P: the kinase is itself regulated through binding χ copies of E^* [78,62,63,61].

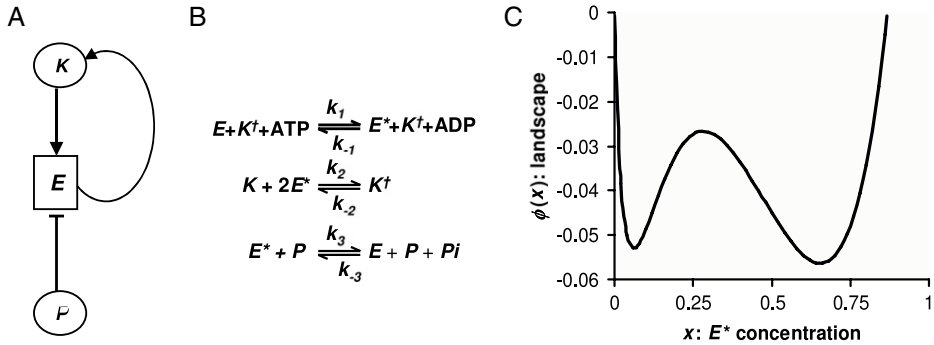

Fig. 15. (A) A simple biochemical signaling network consisting of a regulatory factor E, its activator K (kinase) and inhibitor P (phosphatase). There is a positive feedback from the activated E to the kinase K. The feedback is in the form of activation of the kinase to become $K^\dagger$, shown in (B), by binding of two phosphorylated regulator E^*. (C) The landscape $\phi(x)$ for the network in (A) and (B), with $x_t = 1$, $\alpha = 43$, $\beta = 10$, $\epsilon = 0.01$ and $\delta = 0.5$. The fixed points are at 0.05 (stable), 0.632 (stable), and 0.368 (unstable), corresponding to the two wells and the barrier.

cellular signaling network in Fig. 14(B), with slow fluctuating kinase activity, also exhibit stochastic bistability [76,77]. The theory we present here is indeed general to both types of biochemical networks, with and without gene expression.

If the copy numbers of the molecules are large, then the CME automatically yields the deterministic kinetics as predicted by the traditional kinetic theory. The new information one obtains from the CME is the adaptive landscape shown in Fig. 15(C), which is an emergent entity not given *a priori*. There are two issues related to this important distinction: (1) The mathematical existence of such a landscape in a general, stochastic dynamics which does not have detailed balance; and (2) How is such a landscape, even exists, related to the dynamics, both deterministic and stochastic. The most nontrivial issue here is the logical relationship between the landscape and the dynamics [79,51,80–82]: It is absolutely clear that in the detailed-balanced system, the landscape exists *a priori* and the dynamics is a consequence of the landscape. However, for system without detailed balance, the dynamics, as defined by the reaction networks and all the individual rate constants, define the overall dynamics as well as define the landscape. Hence, logically, it is not correct to say that the dynamics is a consequence of the landscape. Nevertheless, the landscape is still a very useful device to understand and characterize the overall dynamics. The concept of adaptive landscape, thus, should only be understood in this "retrospective" way.

Further, Fig. 15 also suggests that there are three distinct time scales in a bistable mesoscopic biochemical reaction systems. The first time scale is from the individual biomolecular reactions in Fig. 14. For our theory, they are given in terms of the parameters f, g, h, k in Fig. 14(A) and ks in Fig. 14(B). Millisecond are not unreasonable for this time scale, even though certainly there are much faster and slower biochemical reactions inside a cell. The second time scale is the network relaxation to steady states, as illustrated in the Fig. 15(C) by the downhill dynamics, and the third time scale is the transition rates between the two wells. Both the latter two time scales are *emergent properties* of the biochemical network. We shall call

these three time scales molecular signaling time scale (MSts), biochemical network time scale (BNts), and cellular evolution time scale (CEts), respectively.

The CEts is very sensitive to the number of molecules in the biochemical system, thus, with a given concentrations, the size of the cell volume. It could be shown that with the MSts on the order of milli-and microsecond, and with concentration of E on the order of micromolar, the transition times between the two states in Fig. 15(C) can be as long as thirty thousand years! Hence, the stability of the emergent attractors are extremely stable against spontaneous concentration fluctuations (i.e., intrinsic noise) in the system.

4. Remarks on the theory of nonequilibrium steady state

Nonequilibrium statistical thermodynamics has a very rich history. In this section, we give some remarks on the development of the mathematical theory of nonequilibrium steady state (NESS) from the authors perspective. It is certainly not a researched historical account of the subject. We sincerely apologize for the biased and incomplete discussion, which reflects our own ignorance and brief nature of this review.

The idea of detailed balance was independently proposed in the work of chemist Lewis [3,4], influenced by an observation of Wegscheider [83], and physicist Tolman [1,2]. Note that Lewis' *chemical detailed balance* applies to linear and nonlinear macroscopic chemical reactions, while Tolman's detailed balance is formulated in connection to transition probability. They are different. Bridgman wrote a succinct summary, in 1928, on the principle and its relation to the Second Law and to measurability [84]. The role of measurability in a system's entropy was further elucidated in Refs. [85,86]. More importantly, Bridgman clarified the difference between a steady-state sustained by detailed balance (equilibrium) and by cyclic reactions (NESS), an idea that had already been presented in the original work of Boltzmann's kinetic theory. This distinction was explicitly stated by Klein [87] who also introduced the term "nonequilibrium steady-state". For overdamped systems which include all the chemical reactions in aqueous solution, the Second Law ensures the detailed balance in closed systems. The concept of detailed balance was also an essential ingredient of Onsager's theory, which defined detailed balance in terms of time symmetry $(x, v, t) \rightarrow (x, -v, -t)$ [88]. And in the 1950s, Cox formulated a quite complete mathematical theory [89,90], connecting stochastic Markov dynamics based on master equation and Brownian motion with Gibbs' statistical mechanics as well as Onsager's theory of linear irreversibility.

The idea on quantifying entropy increase and the Second Law in irreversible processes first appeared in the work of Eckart [91,92] who related the rate of entropy change to heat dissipation associated with the various linear transport laws, such as that of Ohm (electricity), Fourier (heat), and Newton (viscosity). Again, Bridgman summarized the state of affair [93] and clarified the important equation for "increase of entropy in the region within a closed surface" (dS/dt) and the difference between "entropy which has flowed out of the region across the surface" (hdr) and "entropy generated by irreversible processes within the surface" (epr). Since then, the equation for entropy balance became the center piece of the theory of irreversible thermodynamics [94]. The development of far-from equilibrium open-system theories of Hill [95,96] and the Brussels school [97,70] in the 1970s were both built on these foundations. While the former clearly identified the breakdown of detailed balance and cycle flux with a NESS, the latter emphasized the central role of positive entropy production and the nonlinear nature of self-organization. It is unfortunate that the Cox's stochastic nonequilibrium dynamics had not survived to these later theories which were clearly motivated by chemistry and biology.

Inside mathematics, the legacy of Kolmogorov [5] has been carried on, though in a rather slow pace, in both theory of stochastic processes in connection to symmetric Markov processes [98,99] and statistics in connection to Monte Carlo methods for simulation [100,101]. The monograph [26] was the attempt to introduce rigorously the notions of the NESS and entropy production to mathematicians. The goal of the present review is to re-connect this unifying approach to biophysics and biochemistry. In recent years, an attempt to introduce the stationary cycle flux into the *landscape theory* [7] has also appeared [79,81]. In a nonequilibrium steady state, this is an emergent dynamic aspect that is completely absent in an equilibrium steady state.

References

[1] R.C. Tolman, Phys. Rev. 23 (1924) 693.
[2] R.C. Tolman, Proc. Natl. Acad. Sci. USA 11 (1925) 436.
[3] G.N. Lewis, Proc. Natl. Acad. Sci. USA 11 (1925) 179.
[4] G.N. Lewis, Science 71 (1930) 569.
[5] A. Kolmogorov, Math. Ann. 112 (1936) 155.
[6] H. Kramers, Physica 7 (1940) 284.
[7] H. Frauenfelder, S.G. Sligar, P.G. Wolynes, Science 254 (1991) 1598.
[8] D.D. van Slyke, G.E. Cullen, J. Biol. Chem. 19 (1914) 141.
[9] J. Ninio, Proc. Natl. Acad. Sci. USA 84 (1987) 663.
[10] W. Min, I.V. Gopich, B.P. English, S.C. Kou, X.S. Xie, A. Szabo, J. Phys. Chem. B 110 (2006) 20093.
[11] H. Qian, Biophys. J. 95 (2008) 10.
[12] J.E.M. Hornos, D. Schultz, G.C.P. Innocentini, J. Wang, A.M. Walczak, J.N. Onuchic, P.G. Wolynes, Phys. Rev. E 72 (2005) 051907.
[13] A.M. Walczak, J.N. Onuchic, P.G. Wolynes, Proc. Natl. Acad. Sci. USA 102 (2005) 18926.
[14] P.-Z. Shi, H. Qian, J. Chem. Phys. 134 (2011) 065104.
[15] H. Feng, B. Han, J. Wang, J. Phys. Chem. B 115 (2011) 1254.
[16] H.P. Lu, L. Xun, X.S. Xie, Science 282 (1998) 1877.

[17] X.S. Xie, H.P. Lu, J. Biol. Chem. 274 (23) (1999) 15967.
[18] X.S. Xie, Single Mol. 2 (4) (2001) 229.
[19] B. English, W. Min, A.M. van Oijen, K.T. Lee, G. Luo, H. Sun, B.J. Cherayil, S.C. Kou, X.S. Xie, Nat. Chem. Biol. 2 (2006) 87.
[20] H. Ge, J. Phys. Chem. B 112 (2008) 61.
[21] H. Qian, X.S. Xie, Phys. Rev. E 74 (2006) 010902.
[22] C. Jia, X.F. Liu, M.P. Qian, D.Q. Jiang, Y.P. Zhang, 2010. arxiv:1008.4501.
[23] J.J. Hopfield, Proc. Natl. Acad. Sci. USA 71 (1974) 4135.
[24] J. Ninio, Biochimie 57 (1975) 587.
[25] H. Qian, J. Phys.: Condens. Matter. 17 (2005) S3783.
[26] D.Q. Jiang, M. Qian, M.P. Qian, Mathematical Theory of Nonequilibrium Steady States, in: Lecture Note in Mathematics, vol. 1883, Springer-Verlag, Berlin, Heidelberg, 2004.
[27] N. Carter, R. Cross, Nature 435 (2005) 308.
[28] A.B. Kolomeisky, E.B. Stukalin, A.A. Popov, Phys. Rev. E 71 (2005) 031902.
[29] W. Min, L. Jiang, J. Yu, S.C. Kou, H. Qian, X.S. Xie, Nano Lett. 5 (2005) 2372.
[30] G. Crooks, Phys. Rev. E 60 (1999) 2721.
[31] C. Jarzynski, J. Stat. Phys. 98 (2000) 77.
[32] H. Ge, D.Q. Jiang, J. Phys. A 40 (2007) F713.
[33] E. Sevick, R. Prabhakar, S. Williams, D. Searles, Annu. Rev. Phys. Chem. 59 (2008) 603.
[34] T. Hatano, S. Sasa, Phys. Rev. Lett. 86 (2001) 3463.
[35] H. Qian, D.A. Beard, IEE Proc. Sys. Biol. 153 (2006) 192.
[36] H. Qian, J. Phys. Chem. B 141 (2010) 16105.
[37] A. Cornish-Bowden, Fundamentals of Enzyme Kinetics, Portland Press, London, 2004.
[38] M. Vellela, H. Qian, J. R. Soc. Interface 6 (2009) 925.
[39] J. Botts, M. Morales, Trans. Faraday Soc. 49 (1953) 696.
[40] C. Frieden, J. Biol. Chem. 245 (1970) 5788.
[41] G.R. Ainslie, P.S. Jonathan, K.E. Neet, J. Biol. Chem. 247 (1972) 7088.
[42] W. Min, L. Jiang, X.S. Xie, Asian J. Chem. 5 (2010) 1129.
[43] J.T. Wong, C.S. Hanes, Can. J. Biochem. Physiol. 40 (1962) 763.
[44] D. Nicholls, S. Ferguson, Bioenergetics, 3rd ed., vol. 3, Academic Press, New York, 2002.
[45] E.H. Fischer, L.M.G. Heilmeyer, R.H. Haschke, Curr. Top. Cell. Regul. 4 (1971) 211.
[46] E.G. Krebs, Curr. Top. Cell. Regul. 18 (1980) 401.
[47] J. Howard, Mechanics of Motor Proteins and the Cytoskele, Sinauer Associates, Sunderland, MA, 2001.
[48] J.M. Jeremy, L. Tymoczko, L. Stryer, Biochemistry, 6th ed., W.H. Freeman, New York, 2006.
[49] H. Qian, Annu. Rev. Phys. Chem. 58 (2007) 113.
[50] H. Ge, M. Qian, J. Comput. Biol. 16 (2009) 119.
[51] J. Wang, K. Zhang, E.K. Wang, J. Chem. Phys. 129 (2008) 135101.
[52] A.V. Hill, J. Phys. 40 (1910) iv.
[53] D.E. Koshland, A. Goldbeter, J.B. Stock, Science 217 (1982) 220.
[54] A. Goldbeter, D.E. Koshland, Proc. Natl. Acad. Sci. USA 78 (1981) 6840.
[55] C.F. Huang, J.E. Ferrell, Proc. Natl. Acad. Sci. USA 93 (1996) 10078.
[56] E.H. Fischer, E.G. Krebs, J. Biol. Chem. 216 (1955) 121.
[57] H. Qian, Biophys. Chem. 105 (2003) 585.
[58] H. Ge, M. Qian, J. Chem. Phys. 129 (2008) 015104.
[59] J. Wyman, S.J. Gill, Binding and Linkage: Functional Chemistry of Biological Macromolecules, Univ. Sci. Books, Mill Vally, CA, 1990.
[60] E.M. Ozbudak, M. Thattai, H.N. Lim, B.I. Shraiman, A. van Oudenaarden, Nature 427 (2004) 737.
[61] J.E. Ferrell, W. Xiong, Chaos 11 (2001) 227.
[62] J.A. Cooper, H. Qian, Biochemistry 47 (2008) 5681.
[63] H. Zhu, H. Qian, G. Li, PLoS ONE 5 (2010) e9226.
[64] H. Qian, J. Stat. Phys. 141 (2010) 990.
[65] P. Ao, D. Galas, L. Hood, X.M. Zhu, Med. Hypotheses 70 (2008) 678.
[66] D.A. Beard, H. Qian, Chemical Biophysics: Quantitative Analysis of Cellular Systems, in: Cambridge Texts in Biomedical Engineering, 2008.
[67] J. Schnakenberg, Rev. Modern Phys. 48 (4) (1976) 571.
[68] D. Wilkinson, Stochastic Modelling for Systems Biology, Chapman and Hall, CRC, 2006.
[69] T.G. Kurtz, J. Chem. Phys. 57 (1972) 2976.
[70] G. Nicolis, I. Prigogine, Self-Organization in Nonequilibrium Systems: From Dissipative Structures to Order Through Fluctuations, Wiley, New York, 1977.
[71] J.D. Murray, Mathematical Biology, third ed., Springer, New York, 2002.
[72] J. Monod, J.P. Changeux, F. Jacob, J. Mol. Biol. 6 (1963) 306.
[73] J. Monod, J. Wyman, J.P. Changeux, J. Mol. Biol. 12 (1965) 88.
[74] D.E. Koshland, G. Nemethy, D. Filmer, Biochemistry 5 (1966) 365.
[75] G. Adair, J. Biol. Chem. 63 (1925) 529.
[76] L.M. Bishop, H. Qian, Biophys. J. 98 (2010) 1.
[77] H. Qian, P.-Z. Shi, J. Xing, Phys. Chem. Chem. Phys. 11 (2009) 4861.
[78] J.E. Ferrell, E.M. Machleder, Science 280 (1998) 895.
[79] J. Wang, L. Xu, E.K. Wang, Proc. Natl. Acad. Sci. USA 105 (2008) 12271.
[80] H. Ge, H. Qian, Phys. Rev. Lett. 103 (2009) 148103.
[81] J. Wang, K. Zhang, E. Wang, J. Chem. Phys. 133 (2010) 125103.
[82] H. Ge, H. Qian, J. R. Soc. Interface 8 (2011) 107.
[83] R. Wegscheider, Z. Phys. Chem. 39 (1902) 257.
[84] P.W. Bridgman, Phys. Rev. 31 (1928) 101.
[85] R.M. Noyes, J. Chem. Phys. 34 (1961) 1983.
[86] I.W. Richardson, Eur. Biophys. J. 17 (1989) 281.
[87] M.J. Klein, Phys. Rev. 97 (1955) 1446.
[88] L. Onsager, Phys. Rev. 37 (1931) 405.
[89] R.T. Cox, Rev. Modern Phys. 22 (1950) 238.
[90] R.T. Cox, Rev. Modern Phys. 24 (1952) 312.
[91] C. Eckart, Phys. Rev. 58 (1940) 267.
[92] C. Eckart, Phys. Rev. 58 (1940) 269.
[93] P. Bridgman, Phys. Rev. 58 (1940) 845.
[94] S.R. de Groot, P. Mazur, Nonequilibrium Thermodynamics, North Holland, Amsterdam, 1962.
[95] T.L. Hill, Free Energy Transduction in Biology: The Steady-State Kinetic and Thermodynamic Formalism, Academic Press, New York, 1977.
[96] T.L. Hill, Free Energy Transduction and Biochemical Cycle Kinetics, Springer-Verlag, New York, 1995.
[97] P. Glansdorff, I. Prigogine, Thermodynamic Theory of Structure, Stability and Fluctuations, Wiley-Interscience, London, New York, 1971.
[98] K.-L. Chung, J.B. Walsh, Markov Processes, Brownian Motion, and Time Symmetry, second ed., Springer, New York, 2005.
[99] M.L. Silverstein, Symmetric Markov Processes, in: Lecture Notes in Mathematics, vol. 426, Springer-Verlag, New York, 1974.
[100] N. Metropolis, A.W. Rosenbluth, M.N. Rosenbluth, A.H. Teller, E. Teller, J. Chem. Phys. 21 (1953) 1087.
[101] J.S. Liu, Monte Carlo Strategies in Scientific Computing, corrected ed., Springer, New York, 2008.